In-vivo imaging of tumor-infiltrating immune cells

Zeelen, Carolien; Paus, Carmen; Draper, Derk; Skamp, Sandra He; Signore, Alberto; Gali, Filippo; Ssinger, Cristoph M. Grie; Aarntzen, Erik H.

Published in:
Quarterly Journal of Nuclear Medicine and Molecular Imaging

DOI:
10.23736/S1824-4785.17.03052-7

Publication date:
2018

The Quarterly Journal of Nuclear Medicine and Molecular Imaging 2018 March;62(1):56-77
DOI: 10.23736/S1824-4785.17.03052-7

REVIEW

HYBRID IMAGING IN INFLAMMATION AND INFECTION

In-vivo imaging of tumor-infiltrating immune cells: implications for cancer immunotherapy

Carolien ZEELEN [1], Carmen PAUS [1], Derk DRAPER [1], Sandra HESKAMP, Alberto SIGNORE [2, 3], Filippo GALLI [2], Cristoph M. GRIESSINGER [4], Erik H. AARNTZEN [1] *

[1]Department of Radiology and Nuclear Medicine, Radboud University Medical Center, Nijmegen, The Netherlands; [2]Department of Medical-Surgical Sciences and Translational Medicine, Sapienza University, Rome, Italy; [3]Department of Nuclear Medicine and Molecular Imaging, Groningen University Medical Center, Groningen, The Netherlands; [4]Department of Preclinical Imaging and Radiopharmacy, Werner Siemens Imaging Center, Tuebingen, Germany

*Corresponding author: Erik H. Aarntzen, Department of Radiology and Nuclear Medicine, Radboud University Medical Center, Geert Grooteplein 10, 6500HB, Nijmegen, The Netherlands. E-mail: erik.aarntzen@radboudumc.nl

ABSTRACT

Dynamic interactions between tumor cells and immune cells promote the initiation, progression, metastasis and therapy-resistance of cancer. With respect to immunotherapy, immune cell populations such as cytotoxic CD8+ T-cells, CD56+ NK cells and myeloid phagocytic cells play decisive roles. From an imaging perspective, the immune system displays unique challenges, which have implications for the design and performance of studies. The immune system comprises highly mobile cells that undergo distinct phases of development and activation. These cells circulate through several compartments during their active life span and accumulate in rather limited numbers in cancer lesion, where their effector phenotype further diversifies. Given these features, accurate evaluation of the tumor microenvironment and its cellular components during anti-cancer immunotherapy is challenging. *In-vivo* imaging currently offers quantitative and sensitive modalities that exploit long-lived tracers to interrogate, *e.g.* distinct immune cell populations, metabolic phenotypes, specific targets relevant for therapy or critical for their effector function. This review provides a comprehensive overview of current status for *in-vivo* imaging tumor-infiltrating immune cell populations, focusing on lymphocytes, NK cells and myeloid phagocytic cells, with emphasis on clinical translation.

(*Cite this article as:* Zeelen C, Paus C, Draper D, Heskamp S, Signore A, Galli F, *et al. In-vivo* imaging of tumor-infiltrating immune cells: implications for cancer immunotherapy. Q J Nucl Med Mol Imaging 2018;62:56-77. DOI: 10.23736/S1824-4785.17.03052-7)

Key words: Neoplasms - Molecular imaging - Lymphocytes - T-lymphocytes - Natural killer T-cells - Macrophages - Immunotherapy.

Dynamic and reciprocal interactions between tumor cells and immune cells promote the initiation, progression, metastasis and therapy-resistance of cancer. Distinct patterns of tumor-infiltrating immune cell populations have been demonstrated to impact prognosis in most cancer types.[1-3] In the past years, several immunotherapies have successfully been introduced in the clinic aiming to increase the number and activity of tumor-infiltrating immune cells, *e.g.* immune checkpoint inhibitors, adoptive T-cell transfer, chimeric antigen receptor (CAR) T-cells and dendritic cell-based (DC) vaccines. Spectacular clinical successes have been noted for many cancer types, but consistently only a limited subset of patients. Especially in cancer types with high mutation rates, *e.g.* melanoma, non-small cell lung cancer and renal cancer, showed effective responses to immunotherapeutic approaches. In addition to high costs and serious toxicity profiles, the lack of tools to measure the behavior of immune cell populations hampers efficient application of immune therapy.

With respect to immunotherapy, immune cell populations such as cytotoxic CD8+ T-cells, CD56+ NK cells and myeloid phagocytic cells play decisive roles, exemplified in immune checkpoint inhibitor therapy. Target-

ing PD-1/PD-L1 and CTLA4, the presence and function of CD8+ T-cells has shown to be a prerequisite for response,[4-7] perhaps explaining the limited and heterogeneous responses observed in clinical trials.

Accurate evaluation of a highly dynamic and complex process such as anti-cancer immunotherapy, involving multiple immune cell populations with multifaceted roles, is challenging.[8] Factors that will need to be considered include not only the presence and numbers of cells, but also intra-tumoral localization, functional orientation and reciprocal interactions. Moreover, as these factors vary amongst patients and cancer lesions, heterogeneity should be addressed on a whole body scale.[9] Studies that have been able to capture a more comprehensive evaluation of cancer cells, immune cell subsets and their functional orientations have unquestionably led to valuable insights,[10] using quantitative multicolor immunohistochemistry and gene expression profiling of tumor biopsy samples. However, histopathological evaluation requires invasive procedures to obtain a single sample of one metastasis in a single point in time of a patient with a heterogeneous tumor load, and has, therefore, limited potential to optimize immunotherapies in clinical settings.

In-vivo imaging provides a non-invasive alternative for longitudinal evaluation on a whole-body scale, provided that distincT-cell populations can be assessed simultaneously at sufficient sensitivity to detect limited numbers of cells per volume.

Implications for *in-vivo* imaging

From an imaging perspective, the immune system displays unique challenges, which have implications for the design and performance of such studies. The immune system comprises highly mobile cells that undergo distinct phases of development and activation, and circulate through several compartments during their active life span. In a simplistic view, lymphocytes, including CD4+ helper T-cells, CD8+ cytotoxic T-cells and CD56+ NK cells can be regarded as relatively short-lived highly mobile effector cells that proliferate, execute their effector function and then die. To the contrary, macrophages can be referred to as long-lived, less mobile, master regulators of the local immune microenvironment with highly plastic and reversible phenotypes.

Given these features, the complexity of an accurate evaluation of the tumor microenvironment and its cellular components is enormous. *In-vivo* imaging currently offers quantitative and sensitive modalities that exploit long-lived tracers to interrogate metabolic phenotypes, specific targets relevant for therapy or critical for their effector function. This review will highlight these aspects of imaging specific immune cell populations in cancer lesions.

Modalities for *in-vivo* immune cell imaging

A diverse range of molecular imaging techniques and cell-labeling strategies are available for preclinical and clinical studies. Modalities that are currently used in clinical settings include positron emission tomography (PET) and single-photon emission computed tomography (SPECT) radionuclide imaging, as well as non-nuclear imaging techniques *e.g.* magnetic resonance (MR) imaging, ultrasound (US). In preclinical settings, optical imaging techniques, *e.g.* fluorescence (FLI) and bioluminescence (BLI) play an important role, as well as photoacoustic (PA) imaging. The penetration depth of the signals derived from these techniques is currently too low for detection of labeled immune cells in human subjects. The technical properties of these techniques are comprehensively reviewed elsewhere.[11-14]

Current labels for cell labeling

Cell labeling can be performed in two ways: directly and indirectly (Figure 1). For direct labeling of the target cells, the imaging label is stably attached to or entrapped in the cell during *in-vitro* incubation, as reviewed by Wolfs *et al.*[11] Most direct labeling strategies involve radionuclide imaging, however nanoparticle-

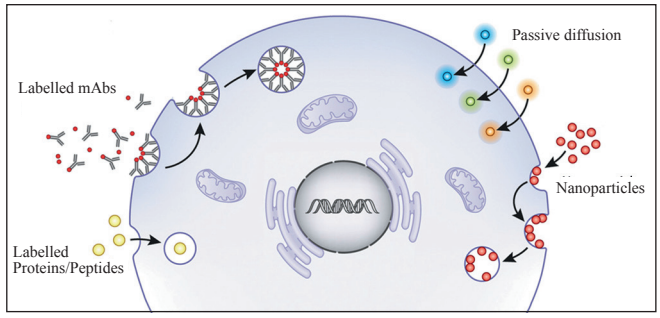

Figure 1.—Currently available direct and indirect cell labeling techniques.

based cell labeling may also apply to other imaging modalities, including MR, US, computed tomography (CT) and optical imaging.

For indirect labeling of cells, imaging reporter gene constructs that encode for receptors or enzymes that specifically will entrap the injectable imaging label *in vivo*, are introduced in the target cells.[15] These techniques mostly apply to radionuclide imaging and optical imaging.

Direct labeling strategies

Direct cell labeling strategies can require incubation of the immune cells with the imaging labeling prior to re-infusion. Advantages of this approach are the lack of background as the imaging label is in principle not present in other host tissues or cells. Furthermore, in general the radioactive dose administered to the subject is low. Its labeling procedure is mostly simple and based on incubation. Lastly, direct labeling does not involve genetic manipulation of the therapeutic cells.

A disadvantage of direct cell labeling is the gradual leakage of most labels from the cells and release of the label from dying cells. This causes uptake of the label by bystander cells or diffusion into the tissue. For *ex-vivo* labeling in clinical studies, particular infrastructure and laboratory facilities are required, which are not common to all centers. Another limitation is the dilution of the intracellular label as cells divide, which might impair detectability. As no new label can be added to the cells after transplantation, the imaging window is at maximum a few half-lives of the label used, which limits the type of questions that can be addressed with direct labeling.

Specific immune cells can also be labeled direct *in vivo*, mostly exploiting the specificity of monoclonal antibodies. Disadvantages of radiolabeled antibodies include the non-specific binding by the cells of the reticulo-endothelial system, predominantly in the liver, spleen and bone marrow. The slow pharmacokinetic properties, *e.g.* long circulation times and slow tissue penetration, of these large proteins often results in an optimal imaging time point a few days after injection, which might not cover processes which physiologically occur at more dynamic rates, such as receptor expression on cell surfaces. The target-to-background ratio is largely dependent on the level of expression, and rate of internalization, of the receptor on the target cell population.

Passive diffusion over the cell membrane

Lipophilic agents like oxine, hexamethyl-propylene amine oxime (HMPAO), pyruvaldehyde-bis-N4-methylthiosemicarbazone (PTSM) and tropolone passively diffuse over the cell membrane, complexes fall apart in the cytoplasm by reduction and the radionuclide dissociates and binds to intracellular proteins. These tracers are amongst the earliest and most widely used techniques for cell labeling.[16, 17]

Cell labeling with ^{111}In-oxine.—In the mid-1970's, ^{111}In-oxine was introduced as a labeling agent for leukocytes; in 1995 it was approved for human use. Although ^{111}In-oxine is routinely used in the clinic for labeling of leukocytes for imaging of infection, mesenchymal stem cells, hematopoietic stem cells as well as CD133$^+$ peripheral blood progenitor cells have been labeled, amongst others. The ^{111}In-oxine solution is in most countries supplied in a vial as a ready-to-use radiopharmaceutical. ^{111}In forms an uncharged pseudo-octahedral N_3O_3 complex with three molecules of 8-hydroxyquinoline (oxine). The complex is neutral and lipophilic, which enables it to penetrate through the bilayer cell membrane. Given the low stability constant of ^{111}In-complexes, cytoplasmic proteins bind ^{111}In and the cell releases 8-hydroxyquinoline. Immune cell labeling with ^{111}In-oxine is in general efficient but some studies have reported gradual efflux of ^{111}In from the cell (up to >60% after 48 hours).[18] A particular concern of ^{111}In-oxine is its direct toxicity. Next to high-energy gamma rays of 171 and 245 keV, ^{111}In also emits low energy Auger electrons that cause damage to the cell.[19-21] ^{111}In-oxine or ^{111}In-tropolone has shown to impair with the proliferative capacity and affects the cell's chromosomal architecture of cytotoxic T-cells. However, viability, phenotype and migration of lymphocytes was not significantly affected.[22, 23]

Cell labeling with ^{99m}Tc-HMPAO.—HMPAO bound to ^{99m}Tc (^{99m}Tc-HMPAO) is the most widely used complex for white blood cell labeling [24] and ^{99m}Tc-HMPAO kit preparations have been commercially available since 1988. Upon reconstitution of the HMPAO kit with ^{99m}Tc-pertechnetate from a fresh generator eluate a lipophilic complex is formed. The lipophilic complex is transformed into free ^{99m}Tc-pertechnetate and a hydrophilic ^{99m}Tc-HMPAO complex in aqueous solution over

time. Freshly-prepared ^{99m}Tc-HMPAO should be used for cell labeling (within 20 minutes of preparation) since only the lipophilic ^{99m}Tc-HMPAO complex can freely cross the cell membrane and is subsequently trapped inside the cell. Two mechanisms have been suggested to be responsible for the retention of ^{99m}Tc-HMPAO inside the cell: 1) conversion of the lipophilic ^{99m}Tc-HMPAO complex into a hydrophilic complex by reducing agents such as glutathione, and 2) binding of ^{99m}Tc-HMPAO to non-diffusible proteins and cell organelles. Some release of ^{99m}Tc-HMPAO from the labeled cells after reinjection into the subject is often observed, resulting in undesired accumulation of radioactivity in the gastrointestinal and urinary tracts. There is little intestinal excretion of ^{111}In-oxine that might have been released by the cells; in the clinical setting planar and SPECT images obtained with ^{111}In-oxine labeled cells are often lower quality than those obtained with ^{99m}Tc-labeled cells, which requires increased acquisition time. The most important disadvantage, however, is the radiation exposure of labeled cells, critical organs (spleen) and the whole body to ^{111}In-oxine, which is substantially higher than that from ^{99m}Tc-HMPAO. Recently, ^{89}Zr-oxine methods have been described in preclinical studies, which would increase the sensitivity of detection and allow quantification by using PET imaging.

Cell labeling with ^{64}Cu-PTSM.—^{64}Cu conjugated to PTSM (^{64}Cu-PTSM) is an intracellular radiolabel for lymphocytes.[25] The redox-active carrier molecule ^{64}Cu-PTSM diffuses passively across the cell membrane because of its lipophilic properties. Within the cytoplasm, Cu(II)-PTSM is reduced to the unstable Cu(I)-PTSM, resulting in the dissociation of Cu(I) from PTSM. The main step of the cell-labeling process is trapping of the released ^{64}Cu, which is subsequently bound by intracellular proteins.[26] Because the positron-emitting radioisotope ^{64}Cu has a half-life of 12.7 hours, non-invasive cell tracking by PET is feasible for several days. Only a few research groups have focused on ^{64}Cu-PTSM labeling of cells for cell-tracking studies.[25, 27, 28] In a detailed characterization of ^{64}Cu-PTSM labeled murine OVA-Th1 cells *in vitro*, an efflux of 53% within 5 hours and 86% within 24 hours after labeling with 0.7 MBq of ^{64}Cu-PTSM was observed. In other cell types, Adonai *et al.* performed efflux studies with rat glioma cells and detected an efflux of 62% within 5 hours and 78% within 24 hours after the labeling procedure.[25] Prince *et al.* reported an efflux of 20% from human dendritic cells within the first hour after ^{64}Cu-PTSM labeling but did not provide efflux rates at later time points. In murine Th1 cells labeled with 0.7 MBq of ^{64}Cu only a slight reduction in viability, IFN-γ secretion, and cell proliferation and an induction of phosphorylated γ-H2AX histones was observed. In contrast to Adonai *et al.*, who proposed the hypothesis that ^{64}Cu is mainly retained in the cytoplasm, Griessinger *et al.* also found ^{64}Cu in the cell nucleus.[28] The double-strand breaks might be caused by the localized radiation within the nucleus because ^{64}Cu decays in 40% by electron capture, emitting Auger electrons that are radiotoxic to DNA.[29]

Cell labeling with ^{111}In-tropolone.—As an alternative to oxine, immune cells have been labeled with ^{111}In-tropolone for clinical use. More recently, mesenchymal stem cells isolated from bone marrow were incubated with ^{111}In-tropolone (15-800 Bq/cell).[17, 30, 31] The labeling efficiency was approximately 25%, yielding 30 Bq/cell. Within the range 15-260 Bq/cell, doubling time was not impaired. However, when using a threefold higher dose, the cell proliferation was completely inhibited, likely caused by cell death as noted from the increased leakage of ^{111}In from the cells. With lower doses, the leakage of ^{111}In from the cells was constant indicating no induction of cell damage. Using 30 Bq/cell it was possible to label mesenchymal stem cells to a level relevant for clinical scintigraphy, without affecting phenotype and differentiation capacity.

Passive incorporation in the cell membrane

The cell surface membrane is a mosaic of reactive groups that allow binding with radiometals and their chelator, for example amino-acid residues and thiol groups. Such approach to cell labeling, hence not specific for the cell type, should result in fewer interactions with intracellular proteins and processes. Recently, several approaches have been reported with high clinical translational potential.

Cell labeling with ^{89}Zr-DBN.—Desferoxamine binds stable to free amino-acid residues, also present on the outer cell membrane. A novel cell labeling agent, ^{89}Zr-desferoxamine-NCS (^{89}Zr-DBN), was synthesized.

Several cell types, including human immune cells, were covalently labeled with ^{89}Zr-DBN *via* the primary amine groups present on cell surface membrane proteins, with a labeling efficiency of 30% to 50% after 30 min labeling depending on cell type. Radioactivity concentrations of labeled cells of up to 0.5 MBq/10^6 cells were achieved without a negative effect on cellular viability. Cell efflux studies showed high stability of the radiolabel, with virtual no loss of tracer up to 7 days, also the *in-vivo* stability of the radiolabel on the human mesenchymal stem cells was demonstrated.[32]

Cell labeling with ^{18}F-HFB.—Ma *et al.* report a simple method for cell labeling with ^{18}F, which involves hexadecyl-4-fluorobenzoate (HFB); a lipophilic long-chain ester that is absorbed in the cell membrane without entering the cytoplasm, in a similar fashion to fluorescent dyes used for cell labeling. Cell labeling efficiency in rat mesenchymal cells was 25% after 30 min; but longer incubation times were not investigated. Cell viability following radiolabeling was found to be >90%, with retention >90% over a 4-hour period.[33] The *in-vivo* distribution of cells labeled with ^{18}F-HFB was followed for 60 min and showed typical distribution pattern to the lungs, and no uptake of radioactivity outside the lung was observed, supporting efficient retention of the radiolabel in the cells. In contrast, injection of the labeling agent itself, ^{18}F-HFB, showed almost complete deposition of radioactivity in the lower abdomen, likely representing the organs of metabolism and clearance (liver, kidneys).

Cell labeling with ^{18}F-FBEM.—Several cell types express thiols at their cell surface. Maleimides derivatives are well-known thiol scavengers and resulted therefore in the generation of ^{18}F-labeled maleimides.[34] ^{18}F-FBEM (^{18}F-4-fluorobenzamido-N-ethylamino-maleimide) reacts quickly and efficient with thiols expressed on the cell and is highly retained in cells up to pH 9.

Active uptake via endogenous transporters.

Cell labeling with ^{18}F-FDG.—Activated proliferating lymphocytes rapidly switch to aerobic glycolysis, which results in increased glucose uptake. This is facilitated by the increased localization of the glucose transporter (Glut1) to the plasma membrane [35] and can be exploited by the most widely used tracer in nuclear medicine, 2-deoxy-2-fluoro-D-glucose (FDG). After entering the cell *via* the Glut-transporter family, phosphorylation by hexokinase 6 results in trapping and accumulation of the tracer in the cell.[36] As tumor cells exploit the same metabolic pathways, *ex-vivo* labeling is unavoidable to discriminate ^{18}F-FDG labeled cells from physiologic background glycolysis or uptake by tumor cells. However, the short half-life of ^{18}F limits its application to image processes that in general span hours to days like accumulation of immune cells in inflammatory lesion. Moreover, efflux of ^{18}F-FDG from cells can be decreased pharmacologically, for example in neural stem cells by using phloretin,[37] but leakage of ^{18}F-FDG from the cells hampers its use in clinical studies.

Active uptake *via* endocytic pathways

Most cells of the myeloid lineage mostly have intrinsic capacity to phagocyte nano-sized compounds from their environment. This characteristic is exploited to label cells with nanoparticles containing an imaging contrast agent. Nanoparticles are a common denominator for engineered particles of 10-1000 nm in size, with a plethora of different coatings, formulations and contents, both for diagnostic or therapeutic purposes.[38-40] For example, (ultra)small paramagnetic iron oxide (U) SPIO nanoparticles are used for labeling phagocytic cells both *in vivo* for improved lymph node staging [41] and *ex vivo* to track therapeutic cells.[42] Stannous chloride colloids have been as carrier for radionuclides to more specifically target monocytes, granulocytes or stem cells.[43]

Cell labeling with ^{99m}Tc-SnF_2.—Phagocytosis of radioactive colloids has attracted considerable interest as a simple method for labeling monocytes and granulocytes with gamma emitting radionuclides for clinical studies. Attempts have been made to label leukocytes not only with a ^{99m}Tc-sulphur colloid.[44, 45] Schroth *et al.* first used ^{99m}Tc-SnF_2 colloids for labeling leukocytes in the whole blood.[43] Labeling efficiency is significantly higher when leukocytes are labeled *in vitro* with ^{99m}Tc-SnF_2 compared with ^{99m}Tc-HMPAO. This can be explained by the different uptake mechanisms. ^{99m}Tc-SnF_2 is taken up by neutrophils and monocytes by phagocytosis, which might well be less for non-phagocytic cells

types like lymphocytes. The size and nature of radiolabeled colloids are important parameters to obtain optimal phagocytosis with minimal surface adsorption.[46, 47]

Active uptake *via* specific receptors

Cell labeling using chemo- and cytokines.—In general, small biological molecules show rapid targeting with high affinity and rapid clearance from circulation. Moreover, most molecules are internalized by their target cells, all-contributing to high target-to-background ratios. Disadvantages include tracer-specific biodistribution with high uptake in physiological sites, often immune-reactive sites. The agent might be biologically active, which may lead to side effects in some cases, which may limit its application in clinical studies.[48]

Cell labeling using monoclonal antibodies.—Receptor expression on the cell surface is mostly dynamic and involves internalization. *In-vivo* or *ex-vivo* binding these receptors may facilitate the radiolabeling of specific cell populations, *e.g.* ^{64}Cu conjugate monoclonal antibodies specific for T-cell receptors of CD4$^+$ T-cells,[28] or ^{89}Zr conjugated diabodies specific for CD8.[49] Both radionuclides have been studied for tracking human peripheral stem cells using anti-CD45 antibodies.[50]

The main advantage of monoclonal antibodies (mAbs) is the high specificity and affinity for their cognate antigen. However, due to their large size, mAbs have a long circulation time and slowly accumulate in the target tissue, imaging should be performed between 6-24 hours post-injection in mice, and 3-5 days post-injection in patients to obtain a high target/background ratio. Disadvantages of radiolabeled mAbs include their sustained background levels and their nonspecific accumulation due to the EPR effect. mAbs can have a mouse origin and can lead to the induction of human anti-mouse antibodies (HAMA) that affect targeting efficiency. However, currently used mAbs are humanized which circumvents this possible adverse effect.

^{89}Zr-based immune-PET imaging has demonstrated a higher stability *in vivo* as compared to ^{124}I-labeled antibodies and has shown feasibility to monitor cancer treatment. ^{89}Zr matches pharmacokinetics of antibodies and provides high-resolution imaging. However, an appropriate chelator system is needed to prevent detachment from antibodies. Several used chelators, such as diethylenetriaminepentaacetic acid (DTPA), ethylenediaminetetraacetic acid (EDTA), 1,4,7,10-tetraacetic acid (DOTA), showed limited stability. DFO has demonstrated to be the most promising with a release of less than 0.2% of Zr^{4+} after 24 hours in serum.[51] However, *in-vivo* stability of ^{89}Zr-DFO labeled antibodies remains an issue and studies have focused on improving DFO linkage to the antibody. An effective approach to conjugate DFO to antibodies is modification of DFO by *N*-succinimidyl-S-acetylthioacetate (SATA), which binds to antibodies after introduction of maleimide moieties. Recently, a novel chelator for DFO* was reported that shows superior stability and *in-vivo* performance compared with DFO.[52]

Indirect radiolabeling strategies

Indirect cell labeling strategies are based on the introduction of a gene construct in the host cell that either encodes for a specific receptor for uptake of the tracer, or for a specific enzyme necessary to entrap the tracer intracellular. The indirectly labeled cells should exhibit enhanced and specific uptake of the injectable tracer once transplanted, which increases detectability as compared to the background. Furthermore, as it requires intact intracellular machinery, it only images viable cells. The transcription can be placed under the control of specific promotors, which allow transcription under predefined conditions. Also, multiple genes can be inserted, only limited by the maximum length of the construct, which potentially allow transfecting cells for multimodal imaging. Lastly, the transfected gene should be passed on to daughter cells, thus cell proliferation does not result in dilution of the label and longitudinal imaging with tracers with short half-life is possible.

Disadvantages of indirect cell labeling include the need for genetic modification, which require regulatory aspects and high level of specific infrastructure, facilities and expertise. Moreover, the level of expression of the vector cannot be controlled, both overexpression and silencing can occur with unwanted effect on imaging. Indirect labeling strategies are currently not being used routinely in clinical studies.

The use of imaging modality specific reporter genes to visualize cells *in vivo* is a common strategy in preclinical studies and was summarized in various reviews.[53, 54] Briefly, most studies use the luciferase reporter gene

and fluorescence proteins (green or red fluorescence protein) for bioluminescence or fluorescence optical imaging. The ferritin receptor and the transferrin receptor represent reporter genes, which can be applied to visualize cells by MRI.[55]

Cell imaging using HSV1-tk reporter genes

Besides, several reporter gene strategies are available for SPECT and PET, which mainly comprises enzymes (herpes-simplex virus thymidine kinase 1; HSV1-tk), receptors (dopamine D2 receptor, somatostatin receptor) or transporters (sodium-iodine symporter, NIS). The application of the HSV1-TK in combination with specific substrates 9-[4-^{18}F-3-(hydroxymethyl)butyl] guanine (^{18}F-FHBG), 2-deoxy-2-^{18}F-5-ethyl-1-D-arabinofuranosyluracil (^{18}F-FEAU) or 2-deoxy-2-^{18}F-5-iodo-1-D-arabino-furanosyluracil (^{18}F-FIAU) is the most commonly used reporter gene system to visualize cells by PET. The HSV1-tk represents also a suicide gene to target transfected cells with the virostatic agent ganciclovir, because the enzyme is naturally not expressed in eukaryotic cells. This represents also one drawback, as the HSV1-TK will be recognized as foreign antigen by the human immune system, which will result in an elimination of the therapeutic transferred cells by the host immune system. The substrates for the HSV1-TK are most likely taken up by nucleoside transporters, which may influence the cellular uptake due to the number of expressed transporters on the cell membranes. Once, the substrate has entered the cell, it will be phosphorylated by the HSV1-TK and thus is trapped within cells.[56]

Cell imaging using NIS reporter genes

Another common example for a PET/SPECT reporter gene is NIS, which is originally expressed in a few human tissues (*e.g.* thyroid). By the application of ^{124}I for PET, ^{125}I for SPECT or other tracers (*e.g.* ^{99m}Tc-pertechnetate) the cells can be visualized due to the active uptake of the radioactive iodine. However, the stability of the tracer within the cells is not very high because no active trapping occurs in the cells. Furthermore, due to its natural occurrence in human tissue, the NIS will be not immunogenic.

A general clinical application of genetically modified cells is currently limited to specialized clinics, due to strict governmental regulations in the use of genetic modified organisms in humans. However, advanced viral vectors for a safe transduction are currently under development and will allow a routine use of genetically modified cells, *e.g.* CAR-T-cells, in patients, and may facilitate also the use of reporter genes for imaging.

Imaging tumor-infiltrating lymphocytes

Passive diffusion over the cell membrane

Cell labeling with ^{111}In-oxine

The robustness of the ^{111}In-oxinate (half-life 2.8 days) cell labeling protocols has resulted in routine application to migration and homing of ^{111}In-oxine labeled T-cells in normal conditions, inflammation and tumor environment.[48] In a clinical study of 35 patients with Hodgkin's disease, ^{111}In-oxine labeling was exploited to investigate the relative CD4$^+$ T-cell lymphocytopenia observed in the majority of these patients. Median 1.0×10^9 (range 0.2 to 2.6×10^9) labeled lymphocytes were re-infused with median 6.3 MBq (range 1.9 to 12.3 MBq) ^{111}In in 17 procedures. ^{111}In-oxine-labeled T-cells accumulated in 54 of 61 lymphoma localizations in enlarged lymph nodes, resulting in increased clearance from the blood pool in patients with active disease as compared to patients in remission,[57] supporting the concept of specific sequestration of CD4$^+$ T-cells in lymphoma lesions.

The preferential accumulation of *ex-vivo* expanded tumor-infiltrating lymphocytes (TIL) was studied in 6 melanoma patients with adoptively transferred ^{111}In-oxine labeled TIL. After cyclophosphamide pre-treatment, 4.4 to 13×10^9 radiolabeled cells were re-infused with 8.6 to 14.8 MBq ^{111}In. Serial scintigraphy imaging showed progressive accumulation of ^{111}In-oxine labeled TIL from 24 hours to 115 hours post-injection in most lesions, varying from 3 to 40 times background level.[58] The same group studied in 18 melanoma patients treated with cyclophosphamide preconditioning and IL-2 injections after adoptively transferred TILs, the tumor-infiltrating capacities of TILs as compared to unselected peripheral blood lymphocytes (PBL).[59] A wide range of 4.4 to 14×10^9 cells were re-infused with 55 to 255 kBq/10^8 cells ^{111}In, and the authors noted a remarkable difference in tumor-infiltration as TILs accumulated in melanoma lesions on 13/18 scans and PBLs only in 1/4 scans.

Pittet *et al.* showed that ^{111}In-oxine labeled cytotoxic T-cells (CTL), allows semi-quantitative assessment and localization of CTL in a mouse model, bearing both hemagglutinin (HA)-negative and HA-expressing tumors. ^{111}In-oxine labeled CTLs specific for HA redistributed to HA-expressing tumors after 2 hours with continuous increase for up to 120 hours post-injection. Moreover, HA-specific CTL localized centrally in HA-positive tumors, as opposed to CTL in HA-negative tumors, which remained at the periphery of the tumor. These findings are consistent with earlier observations by intravital microscopy which showed the requirement of tumor specific antigen expression for deep infiltration of CTL.[60]

Cell labeling with ^{99m}Tc-HMPAO

^{99m}Tc-HMPAO labeling has not been employed for the study of tumor-infiltrating lymphocytes, likely because the shorter half-life of ^{99m}Tc (6 hours) as compared to ^{111}In (2.8 days). However, in a preclinical model of subcutaneous injections of OVA-pulsed or non-pulsed dendritic cells that migrate to the inguinal lymph nodes, it was noted that ^{99m}Tc-HMPAO labeled OVA-specific CD4$^+$ T-cells migrate specifically to the lymph nodes that contain OVA-pulsed dendritic cells within 3 hours.[61]

Cell labeling with ^{89}Zr-oxine

Although the relatively long half-life of ^{111}In allows longitudinal tracking of labeled cells in processes that typically require multiple days, the low sensitivity and poor spatial resolution of the gamma camera imaging/SPECT is insufficient for more advanced applications and imaging of scarce cell populations. Recently, several procedures to label cells with ^{89}Zr have been described.[32, 62, 63] These methods offer a potential solution to the emerging need for a long half-life PET tracer for quantitative imaging of immune cells exploiting the improved sensitivity of PET scanners.

^{89}Zr-oxine labeling was demonstrated to not affect CTL survival, proliferation and function. In preclinical models, ^{89}Zr-oxine labeled T-cells (185 kBq/5 $\times 10^6$ cells) first were trapped in the lungs, but subsequently redistributed to spleen, lymph nodes and liver. After 6 hours, ^{89}Zr-oxine labeled CTLs started to accumulate in tumors of a mouse melanoma model, for up to 4.6% of the total injected activity, which significantly resulted in tumor regression at day 7 after injection.[63] Following a different radiochemical approach, ^{89}Zr-oxinate was also used to label other immune cell populations, like human leucocytes.[62]

Cell labeling with ^{64}Cu-PTSM

^{64}Cu-PTSM has been used for extended cell tracking in lymphocytes, which were observed to accumulate in spleen, liver, bone marrow and the tumor site in a mouse glioma model.[25] ^{64}Cu-PTSM labeling of mouse Th1 cells showed to be a highly sensitive method for *in-vivo* monitoring of T-cell homing for up to 48 hours, without affecting critical cell functions. Highest cell viability and labeling efficiency was achieved by labeling OVA-Th1 cells for 3 hours with 0.7 MBq per 1 $\times 10^6$ cells. Intraperitoneal injected OVA-Th1 cells distributed to the perithymic lymph nodes, whereas intravenous injection of ^{64}Cu-OVA-Th1 cells resulted in homing in the lungs and spleen.[28] The accumulation of ^{64}Cu-OVA-Th1 cells in the pulmonary LNs 24 hours after injection was highest in the OVA-immunized and -challenged airway hyperreactivity-diseased mice after intraperitoneal administration. Moreover, ^{64}Cu-OVA-Th1 cells also accumulated significantly in the pulmonary LNs of non-immunized OVA-challenged mice as compared to control mice.

In order to maximize the retention of the ^{64}Cu label, T-cells have been electroporated with ^{64}Cu^{2+} gold nanoparticles and imaging in *in-vivo* models demonstrated high potential in evaluating immunotherapy.[64] This method could circumvent the extended time required for internalization of nanoparticles by endocytosis, which is a practical limitation for radionuclides with short half-life.

In general, these mentioned labeling approaches suffer from a low stability *in vivo*, which limits their applicability for imaging scarce cell populations over prolonged periods of time.

Passive incorporation in the cell membrane

Cell labeling with ^{18}F-FBEM

Covalent binding of functional groups on the cell membrane has the advantage of stable labeling of cells

as long as they are intact, and without perturbing intracellular processes. *Ex-vivo* ^{18}F-FBEM labeling of T-cells has been described with no effect on viability and physiological biodistribution mainly to the spleen, after intravenous injection in a mouse model.[34] In a follow-up study by the same group, in a mouse model for idiopathic pulmonary fibrosis, they demonstrate recruitment of ^{18}F-FBEM labeled leucocytes, predominantly lymphocytes, to the inflamed lung.[65]

Active uptake via endogenous transporters.

Cell labeling using ^{18}F-FDG

Early studies demonstrated a reasonable labeling efficiency of ^{18}F-FDG of approximately 55-70% in lymphocytes (with 30-40 MBq per 2.5 $\times 10^8$ cells). This would allow tracking of the cells for 24-36 hours. However, this strategy precludes long term imaging due to its short half-life of ^{18}F, probe dilution by proliferation and release from the cell by phosphatase activity.[66]

Cell labeling targeting other metabolic pathways

Exploiting metabolic pathways is intrinsically an interesting approach for cell labeling as these processes are in general very efficient, and occurs only in living cells. Furthermore, metabolic profiles reveal the functional orientation of cells, which may provide additional information. Several tracers, with specificity for lymphocyte metabolism, are being developed for *in-vivo* imaging, but have so far not been tested for evaluation of tumor-infiltration. ^{18}F-FLT is a thymidine analogue that correlates with DNA synthesis as it is taken up in the cell where it is phosphorylated by thymidine kinase.[67] In melanoma patients who underwent dendritic cell-based vaccinations, signal intensity of ^{18}F-FLT PET/CT correlated with the lymphocyte response as measured by immune assays in peripheral blood.[68]

Another PET tracer that is selectively incorporated in DNA during synthesis is ^{18}F-1-(2-deoxy- 2-fluoro-D-arabinofuranosyl)thymine (^{18}F-FMAU). Increased radioactivity was detected in fast proliferating tissues, lymph nodes and the bone marrow where it is highly resistant against degradation, indicating its potential to visualize T-cells.[69] A novel probe that specifically targets activated T-cells is the nucleoside analogue 1-(2'-deoxy-2'-^{18}F-fluoroarabinofuranosyl)-cytosine (^{18}F-FAC). Direct *in-vivo* labeling showed enhanced uptake by lymphoid organs and rapidly proliferating tissues in which the salvage pathway is predominant for DNA synthesis. As most other tissues rely on the de novo pathway for DNA synthesis, ^{18}F-FAC showed a more selective uptake in lymphoid organs than other nucleoside metabolism tracers such as ^{18}F-FLT and ^{18}F-FMAU.[69, 70] Proliferating T-cells utilize 10-fold more glutamine than any other amino-acid to regenerate oxaloacetic acid which is consumed by biosynthesis.[35] Magnetic resonance spectroscopy (MRS) and serum analysis of ^{1}H-NMR and ^{19}F-NMR have been used for imaging the bio distribution of T-cells by detecting the metabolites associated with increased glycolysis in inflammation.[71, 72]

Active uptake via endocytic pathways

Because of the low phagocytic activity of T-cells, cationic transfection agents like poly-L-lysine or cell penetrating peptides that enhance endocytosis, like Tat peptides or protamine, are required for sufficient intracellular labeling of imaging tracers. Most studies that exploit endocytosis for cell labeling include single or multimodal imaging tracers which are formulated in (nano)particles.

Cell labeling with ^{89}Zr-chitosan nanoparticles

Chitosan nanoparticles are taken up by cells via various endocytic pathways.[73] Exploiting these mechanisms, chitosan-nanoparticle constructs have been shown to bind ^{89}Zr and thereby deliver ^{89}Zr into human leucocyte populations with labeling efficiencies of 65.5%, for nanoparticles of different molecular weights.

Cell labeling with (ultra) small iron oxide particles

T-cells labeled with small iron oxide particles (SPIO) demonstrated high sensitivity as even single cells could be detected at 9.4T in confined localizations in the subject.[74, 75] In a preclinical study, ovalbumin (OVA) specific lymphocytes labeled with SPIO particles were adoptively transferred into mice with OVA-expressing tumors. More than 95% of cells remained viable after the labeling procedure and did not affecT-cell prolifera-

tion. Twenty-four hours after injection, the signal was increased in the spleen and a significant increased signal was seen in the tumor after 24 hours until 72 hours after injection. The OVA specific T-cells induced regression of OVA-positive tumors compared to OVA-negative tumors.[75] A similar study was done with highly derivatized cross-linked iron oxide nanoparticles (CLIO-HD) that were used to label adoptively transferred T-cells in a melanoma mouse model. High labeling efficiency was achieved without affecting the function of T-cells. 3D MRI showed recruitment of T-cells in the tumor with high resolution.[53, 76, 77]

Cell labeling with ^{19}F-based agents

^{19}F-containing perfluorocarbon (PFC)-based labeling approaches are analogous to those used for SPIO and allow imaging with ^{19}F MR. PFC-based cell tracking enables cell detection with high specificity and allows quantification due to the absence of background signal because of the low concentration of naturally occurring ^{19}F in the body.[74, 78] Cell detection sensitivity is estimated to be in the order of 10^4 to 10^5 cells per voxel in clinical setting.[78]

Cell labeling using multimodal nanoparticles

Dual mode fluorescently labeled PFC allows visualization of the fate and phenotype of the label with fluorescence imaging in addition to MRI. A study that showed that this approach is effective in labeling and subsequent imaging of T-cells used BODIPy-TR PFPE nano-emulsions as dual mode tracer.[79] Confocal microscopy confirmed presence of the nano-emulsion within T-cells. Fluorescence intensity showed a linear correlation with the ^{19}F NMR signal, which demonstrates the potential for using fluorescence imaging for quantification purposes. Injection of labeled $CD4^+$ T-cells showed accumulation to lymph nodes in mice, which was confirmed by isolation of lymph nodes and microscopic analysis of cells.[79]

Another dual mode imaging approach that is promising for *in-vivo* tracking of T-cells in high-resolution MRI makes use of cross-linked iron oxide nanoparticles (CLIO). Tat peptides which are internalized in cells by adsorptive endocytosis, were coupled to CLIO particles that carried a fluorochrome. High labeling efficiency with a prolonged intracellular retention was achieved while low toxicity was reported.[80]

Genetically modified T-cells expressing chimeric antigen receptors (CAR) exert anti-tumor effect by identifying tumor-associated antigens. For maximal efficacy and safety of adoptively transferred cells, *in-vivo* assessment of their biodistribution is critical. This will determine if cells home to the tumor and assist in optimizing cell dosing. A method is developed for loading high cell number with multi-modal (PET-MRI) contrast agents (*e.g.* SPION-^{64}Cu), which could potentially be used for ^{64}Cu-based whole-body PET to detect T-cell accumulation region with high-sensitivity, followed by SPION-based MRI of these regions for high-resolution anatomically correlated images of T-cells. CD19-specific CAR-T-cells labeled with SPION effectively target *in-vitro* $CD19^+$ lymphoma.[81]

Active uptake via specific receptors

Receptor expression on the cell surface is mostly dynamic and involves internalization and/or activation of the downstream signaling pathways. *In-vivo* or *ex-vivo* binding these receptors may facilitate the radiolabeling of specific cell populations

Cell labeling using radiolabeled cytokines and chemokines

Once activated and regulatory T-cells express increased numbers of receptors involved in activation signaling and chemotaxis. Following their physiological role, these mediators often have high affinity for their cognate receptors expressed on inflammatory cells, which renders them interesting candidates for *in-vivo* imaging. The most investigated receptor is the interleukin (IL)-2 receptor, named CD25, highly expressed on activated T-lymphocytes. As early as the 1980's, IL-2 has been labeled with various isotopes, (*i.e.* ^{123}I, ^{125}I, ^{99m}Tc, and ^{18}F) and tested in animal models. Clinical studies using radiolabeled IL-2 involve patients with a wide variety of inflammatory conditions like inflammatory bowel disease, diabetes, atherosclerotic plaques and melanoma patients. Radiolabeled IL-2 is the only cytokine that has been investigated in human cancer. Activated T-lymphocytes show an increased expression of the IL-2 receptor and IL-2 labeling can

therefore be used for T-cell tracking. ^{123}I- and ^{99m}Tc-labeled IL-2 have demonstrated to image lymphocytic infiltration in several inflammatory diseases as well as in melanoma.[82, 83]

Cell labeling using monoclonal antibodies

Several monoclonal antibodies (mAbs) for specific cell types have been used, targeting *e.g.* CD45, CD3, CD4 and CD8.[48] Both PET and SPECT imaging demonstrated to successfully detect T-cell infiltration in a variety of diseases, including infiltration in cancer lesions. Making ultimate use of the specificity of mAbs, this strategy has also been investigated to label T-cell populations expressing a specific T-cell receptor in a preclinical mouse model.[28] Using a T-cell receptor (TCR)-specific labeling approach, Griessinger *et al.* showed that continuous TCR plasma membrane turnover and the endocytosis of the specific ^{64}Cu-mAb-TCR complex enables a stable labeling of T-cells. The TCR-mAb complex was internalized within 24 hours, and no detrimental effects on antigen recognition, viability, DNA-damage and apoptosis or effector function were noted. This approach enabled to follow and quantify the specific homing of systemically applied ^{64}Cu-labeled chicken ovalbumin (cOVA)-TCR transgenic T-cells into the pulmonary and perithymic lymph nodes (LNs) of mice with cOVA-induced airway hyper-reactivity, but in a reduced amount into pulmonary and perithymic LNs of naïve control mice or mice diseased from turkey or pheasant OVA-induced airway hyper-reactivity. This labeling approach is theoretically applicable to other cells with constant membrane receptor turnover and highly interesting for the detection of small numbers of immune cells with preferential homing to specific localizations like lymph nodes and tumor lesions.

The specific targeting of CD25, expressed on activated lymphocytes in leukemia patients is especially interesting as anti-CD25 mAbs have been labeled for diagnostic and therapeutic purposes. Zhang *et al.* demonstrated the potential clinical relevance of the anti-CD25 monoclonal antibody ^{90}Y-labeled 7G7/B6 as a radio-immunotherapy for CD25-expressing lymphomas. ^{111}In-labeled 7G7/B6 significantly accumulated in the tumor of a mouse lymphoma model, with the highest concentration at 48 hours. Mice injected with ^{90}Y-labeled 7G7/B6 showed a prolonged survival as compared to both the untreated mice and the mice injected with an isotype-matched control antibody. Furthermore, total remission occurred in 30% of mice receiving a low dose (2.8 MBq of ^{90}Y labeled 7G7/B6) and 75% in the high-dose group (5.6 MBq), whereas all mice in the control group died.[84]

Cell labeling using antibody fragments

Antibody fragments, such as the diabodies (db) and minibodies (Mb), typically have half-lives that range from 2 to 5 hours and from 5 to 12 hours, respectively. This is an advantage over intact antibodies with half-lives of up to 3 weeks. Although the total uptake in tumors is decreased with antibody fragments, the rapid clearance of engineered antibody fragments still results in higher tumor-to-background ratios at earlier time points. Moreover, antibody fragments lack Fc-effector functions and thus are biologically inert.

^{64}Cu-conjugated minibodies specific for CD8 have been constructed from the variable regions of two anti-murine CD8-depleting antibodies. The minibodies (Mbs) bound to primary CD8$^+$ T-cells from the thymus, spleen, lymph nodes, and peripheral blood. Importantly, this approach did not result in depletion of CD8$^+$ T-cells *in vivo*. In a series of experiments, these ^{64}Cu-radiolabeled Mbs produced high-contrast immuno-PET images 4 hours post-injection and showed specific uptake in the spleen and lymph nodes of antigen-positive mice.[85] By the same group, ^{89}Zr-desferoxamine–labeled anti-CD8 cys-diabodies (^{89}Zr-malDFO-169 cDb) were generated for PET imaging of tumor-infiltrating CD8$^+$ T-cells. Using this tool changes in systemic and tumor-infiltrating CD8 expression were detected in different preclinical syngeneic tumor immunotherapy models, including antigen-specific adoptive T-cell transfer and checkpoint blockade antibody therapy targeting PD-L1.[49]

In another example, human TCR-transgenic T-cells were tracked *in vivo* by directly targeting the murinized constant TCR beta domain (TCRmu) with a ^{89}Zr-labeled anti–TCRmu-F(ab')2 fragment. Using a murine xenograft model of human myeloid sarcoma, the authors monitored the presence of human central memory T-cells, which were transgenic for a myeloid peroxidase-specific TCR. Diverse T-cell distribution patterns were detected by PET/CT imaging, depending on the tumor size and rejection phase. Results were confirmed by im-

munohistochemistry and semi quantitative evaluation of T-cell infiltration within the tumor corresponding to the PET/CT images.[86]

IndirecT-cell labeling approaches for lymphocytes

A PET reporter gene encodes a protein that mediates the specific accumulation of a PET reporter probe (PRP) labeled with a positron-emitting radionuclide. PRGs developed to date encode proteins with various activities, including enzymes, transporters, and receptors.[87] The most commonly used PRGs are based on herpes simplex virus type 1 thymidine kinase (HSV1-tk). Several PRPs can be used to image cells engineered to express HSV1-tk-based PRGs: ^{18}FFHBG, ^{18}F-FEAU and ^{18}F-FIAU. To date, HSV1-tk is the only PRG that has been used to visualize intracerebral injected HSV-TK1 expressing CD8$^+$ T-cells in a patient with glioblastoma by using the substrate ^{18}F-FHBG.[88] The main concern of HSV1-tk as a PRG is its immunogenicity, which can lead to immune-mediated elimination of transfected immune cells. Replacing the viral kinase with a human orthologue might solve this, although such approach introduces other issues concerning the level of expression as compared to normal tissue and possible switch of engineered cells to "suicide mode." Campbell *et al.* developed a mutant PRG enzyme, using structure guided enzyme engineering, which is orthogonal to the wild type enzyme regarding its ability to phosphorylate endogenous nucleosides.[89] This TK2 double mutant efficiently phosphorylates L-^{18}F-FMAU and has lower activity for the endogenous nucleosides thymidine and deoxycytidine than wild type TK2. Imaging studies in mice indicate that the sensitivity of this new human PRG is comparable with that of a widely used PRG based on HSV1-tk. The first clinical studies are awaited.

Human deoxycytidine kinase triple mutant (hdCK-3mut) has been used as a PET reporter by co-expression with the anti-melanoma T-cell receptor F5. *In-vivo* PET imaging enabled monitoring of tumor infiltration without affecting the T-cell function.[90]

Regulatory T-cells (T_{regs}) lines derived from CD4$^+$CD25$^+$FoxP3$^+$ cells have been retrovirally transduced with a construct encoding for the human NIS and the fluorescent protein mCherry. NIS expressing self-specific T_{regs} were radiolabeled *in vitro* with ^{99m}Tc-pertechnetate (^{99m}Tc-O_4^-) and exposure of these cells to radioactivity did not affect cell viability, phenotype or function. Next, adoptively transferred T_{reg}-NIS in C57BL/6 mice were imaged in the spleen after 24 hours.[61]

Moroz *et al.* compare in a recent study the labeling of T-cells by comparing the efficiency of the reporter genes norepinephrine transporter (hNET), human NIS, a human deoxycytidine kinase double mutant (hdCK-DM), and the HSV1-tk. After injection the combination of the hNET and its specific tracer ^{18}F showed the highest sensitivity, detecting 35-40 $\times 10^3$ T-cells *in vivo*.[15]

Imaging tumor-infiltrating NK cells

Passive diffusion over the cell membrane

Direct NK cell labeling can be achieved by using either ^{111}In-oxine or ^{99m}Tc-HMPAO. First studies from Meller *et al.* were performed in patients with renal cell carcinoma. They received 3 to 7 $\times 10^7$ NK cells labeled with ^{111}In-oxine together with a 10-fold excess of unlabeled NK cells obtained from allogeneic donors. Whole body images were obtained 0.5-144 hours post-injection and detected labeled NK cells in two of four large metastases. NK cells were still detected in the blood up to 3 days after injection, as confirmed by PCR, but always in low numbers.[91] Brand *et al.* performed ^{111}In-oxine NK cell scintigraphy in patients with renal cell carcinoma showing their accumulation in 2 out of 4 cancer lesions. Since signal half-life remained almost constant over the 6 days they hypothesized an extended survival of the transfused cells.[92]

Imaging of NK cells generated from umbilical cord blood (UCB) CD34$^+$ hematopoietic progenitor cells for anti-leukemia immunotherapy, has been performed following adoptive transfer in immunodeficient NOD/SCID/IL2Rg(null) mice. A somewhat higher dose of 0.4 MBq of ^{111}In-oxinate was added to 10^6 cells, with labeling efficiency exceeding 80%, cell viability >90% and cell recovery >95%. In addition, this procedure did not affect the migration capacity of UCB-NK cells towards the prototypic BM-chemokine CXCL12 *in vitro*.[93]

Melder *et al.* labeled NK cells with ^{11}C-methyl-iodide to track activated NK cells in a mouse fibrosarcoma model and compare their biodistribution to non-activated splenic lymphocytes. After 30-60 minutes, 4-30% of the injected dose was present in the tumor. Although

variable, this is higher than 3-4% of the non-activated splenic lymphocytes.[97]

A new pre-clinical approach has been applied by Malviya *et al.*, who expanded *in-vitro* murine NK cells and radiolabeled them with ^{111}In-oxine. They showed that labeling with 0.011 MBq of ^{111}In-oxine per 10^6 murine NK cells provided optimal labeling efficiency without affecting cell viability or functionality.[94] A total of 1 $\times 10^6$ freshly isolated and labeled cells were then re-infused in a human lung cancer mouse model. Mice with lung cancer showed higher tumor uptake of labeled NK cells than control mice. Mice that were irradiated showed a decrease of labeled cells in the tumors between 24 hours and 72 hours post-injection, which was accompanied by tumor regression. Non-irradiated mice showed no decrease in labeled cells but also no tumor regression up to 72 hours after injection. As a control, mice that received no NK cells were irradiated and showed a high tumor burden 72 hours after injection, suggesting that the combination of both radiation and NK cell injection has the best antitumor effect in this mouse model.[94]

Passive incorporation in the cell membrane

Despite the lower translational potential in humans, optical imaging can be performed in pre-clinical models to evaluate NK cell trafficking with no radiation exposure to operator. To this purpose, Tavri *et al.* used near-infrared dye DiD (1,19-dioctadecyl-3,3,39,39-tetramethyl-indodicarbocyanine) to label NK cells targeting epithelial cell adhesion molecule antigen in human prostate cancer xenografts in rats.[95] *In-vitro* studies showed a persistence of fluorescent labels over a period of 24 hours without significant change in cell viability. *In-vivo* studies showed a significant increase of fluorescent signal in the xenograft tumors 24 hours after fluorescent NK cell injection as also confirmed by fluorescence microscopy.

Active uptake via endogenous transporters

^{18}F-FDG labeling was also attempted to study the biodistribution of NK-92 cells and NK-92 cells genetically modified to express a chimeric antigen receptor that is specific to the tumor-associated ErbB2 (HER2/neu) antigen. After injection of 5 $\times 10^6$ ErbB2-specific cells into tumor-bearing mice, digital autoradiography showed an increased uptake of radioactivity in HER2/neu-positive tumors. Conversely, the parental NK-92 cells did not accumulate in tumor tissue.[96]

Active uptake via endocytic pathways

Daldrup-Link*et al. et al.* optimized labeling of human NK-92 cells directed against HER2/neu receptors with SPIOs ferumoxide and ferucarbotran in mice with Her2/neu positive mammary tumors imaged with MR.[96] Labeling with both ferumoxide and ferucarbotran (1 $\times 10^6$ cells at a dose of 100-300 µg Fe) was effective using lipofection and electroporation techniques but not in simple incubation. Intracellular cytoplasmic uptake was significantly higher using ferucarbotran. They showed a progressive signal decline in the tumors after injection with these NK cells that were directed against the receptors but not after injection with control NK-92 cells, confirmed by histopathology.

The intra-arterial delivery of SPIO-labeled NK cells (100 pg iron/cell suspensions of FeO label-Texas Red with 4.5 µg/mL protamine sulfate) in hepatocellular carcinoma in rats, was tested by Sheu *et al.* Labeling efficiency was 88±3.1% with a decreased cell viability when using higher SPIO incubation concentrations. This study showed that intra-arterial injection of NK cells permits selective delivery with a significantly increased NK cell dose delivered to the tumor, which can be visualized as T2* measurement reduction using MRI supported by histology.[96]

Meier *et al.* used a similar approach as Tavri *et al.* against epithelial cells in rat xenografts, but used SPIO ferumoxides as labeling technique. In their study 1.5 $\times 10^7$ NK cells were injected intravenously with a significant decline of tumor cells within 24 hour measured using contrast to noise ratio as confirmed by histopathology.[96]

Jang *et al.* demonstrated the use of an external magnetic field using a neodymium magnet to perform near infrared fluorescent imaging of Cy5.5-conjugated Fe_3O_4/SiO_2 nanoparticle-labeled NK cells in mice bearing a human tumor xenograft. This method of applying a magnet on the outside of the tumor increased the infiltration of magnetic NK cells from 2% to 34% within 10 minutes.[104] When the magnet was removed, the cells migrated away from the tumor within minutes caused

by blood flow. Unfortunately, this approach cannot be applied to in deep tumor lesions.

Mallett *et al.* used MRI to track subcutaneously injected NK cells labeled with MoldayION RhodamineB in nude mice with humane prostate cancer. Loss of signal was observed in tumor areas after 24 hours up to 4 days after injection. Histology showed more NK cells in the center of the tumor but this could not be seen in the MRI images.[97]

The use of ^{19}F-PFC has also been explored to label and track NK cells in preclinical models. Human NK cells were expanded with interleukin-2 (IL-2) and labeled *in vitro* with increasing concentrations of ^{19}F-PFC and doses as low as 2 mg/mL ^{19}F were detected. Higher doses of ^{19}F up to 8 mg/mL, led to an improved ^{19}F signal by MRI with 3×10^{11} ^{19}F atoms per NK cell, without affecting cell function. ^{19}F-labeled NK cells were detectable immediately by MRI after intratumoral injection in NSG mice up to 8 days. When ^{19}F-labeled NK cells were injected subcutaneously, a gradual loss of signal at the site of injection suggested their migration to distant organs.[98]

Active uptake via specific receptors

Monoclonal antibodies

A ^{99m}Tc-anti-CD56 mAb has been used to target and follow the trafficking of human NK cells inoculated in SCID mice bearing human cancer. NK cells accumulated in the tumor within 24 hours and were imaged as early as 3 hours after intravenous administration of ^{99m}Tc-anti-CD56. A positive correlation was observed between T/B ratio calculated on tumor lesions and TINKs infiltration. However, no correlation was found between the number of injected NK cells and their number in the tumor. However, larger tumors were more infiltrated and showed more NK cell induced necrosis.[99]

Anti-CD56 antibodies were also used to coat quantum dots for fluorescent imaging of human NK cells.

Indirect labeling of NK cells

In-vivo bioluminescence imaging (BLI) can detect small numbers of cells noninvasively and enables the quantification of tumor growth within internal organs with fusion genes that encode bioluminescent and fluorescent reporter proteins. Such dual function reporter genes have also been used to label effector NK cells and monitor their homing to tumor sites.[100]

Imaging tumor-associated macrophages

Tumor-associated macrophages (TAMs) are a major cell population within the tumor microenvironment, which play a multifaceted role in various stages of tumor progression. Macrophages are functionally plastic and can alter their polarization state to accommodate different physiological conditions. TAMs may originate from tissue-specific mononuclear phagocytic cells, *e.g.* alveolar macrophages, Kupffer cells that reside in the tissue at pre-cancerous stages. However, the majority of TAMs at clinical overt stages of disease originate from recruited circulating monocytes with inflammatory phenotypes [101, 102] and acquire their functional phenotypes by interacting with the tumor microenvironment.[111] At the extremes of their phenotypic continuum, macrophages range from M1 to M2 polarization states: classically activated M1 macrophages produce type I pro-inflammatory cytokines, participate in antigen presentation and have an anti-tumorigenic role. Conversely, "alternatively-activated" M2 macrophages produce type II cytokines, promote anti-inflammatory responses and have pro-tumorigenic functions.

For example, at the leading edge of tumors, TAMs facilitate tumor cell invasion through a paracrine signaling loop that involves tumor-derived colony stimulating factor 1 (CSF-1) and macrophage derived epidermal growth factor (EGF). Beyond the leading edge, TAMs are the major source of proteases; further supporting tumor progression and tumor motility. Furthermore, tumor vascularization requires the co-operation of multiple TME cell types, including TAMs, releasing pro-angiogenic signals into the TME. Similarly, in lymphangiogenesis, another mode of vascularization in tumors and an alternative route for cancer cell dissemination, activated macrophages produce VEGF Beyond the initial acquisition of invasiveness in primary tumors and the contribution to infrastructural vascularization, the next major step in the metastatic cascade is intravasation into circulation. In the tumor core, macrophages localize to blood vessels, where they help tumor cells intravasate into the circulation. Moreover, the density of clusters of TAMs, endothelium and tumor cells correlates with distant metastasis.[103, 104]

From an imaging perspective, the high phagocytic and storage capacity of TAMs allows loading with imaging contrast containing nanoparticles to reach high intracellular concentrations for optimal signal-to-background ratios. Moreover, as these cells hardly proliferate in the tumor microenvironment, label dilution and subsequent loss of signal is less of a problem. Challenging however is to pinpoint specific functional phenotypes that can be present in the tumor-environment simultaneously.

Passive diffusion over the cell membrane

Cell labeling using ^{111}In-oxine

The high abundance of tumor-associated macrophages in renal cell carcinoma prompted studies with therapeutic infusion with monocyte-derived macrophages in renal cell carcinoma patients. Monocytes were differentiated *ex vivo* with granulocyte-macrophage colony-stimulating factor (GM-CSF) and short pulse of IFN-γ for a total of 7 days before re-infusion. To study their tumor homing capacity, Quillien *et al.* labeled these cells applying 15 MBq ^{111}In-oxine per 3 to 10 $\times 10^6$ cells resulting in high labeling efficiency.[105] Upon intravenous injection of approximately 800 $\times 10^6$ labeled cells, only 1 lesion in 15 patients was visualized. Similar findings have been reported in other clinical studies with comparable culture protocols.[106, 107] Detailed phenotyping of the cells after *ex-vivo* culture revealed a granulocyte-like phenotype with expression of CD66, as well as CD14. This might suggest that, although radiolabeling has no effect on macrophage viability and function, the *ex-vivo* culture condition are of major influence on the homing characteristics of monocyte-derived cells.

The *in-vivo* distribution of *ex-vivo* macrophage activated killer (MAK) cells has been studied with *in-vivo* labeling with ^{111}In-oxine and ^{18}FFDG and linking these cells to the bi-specific antibody MDX-H210.[108] Radiolabeled MAK cells were delivered either by IV or intraperitoneal (IP) injection in ten patients with peritoneal relapse of epithelial ovarian carcinoma. Following 8 of 16 IV infusions or 4 of 6 IP infusions the labeled cells were tracked to the tumor lesions. However, the leakage of ^{18}F-FDG limited the ability to confidently confirm the tracking of the MAK cells to the tumor in all cases. The addition of MDX-H210 bi-specific antibody did not alter the distribution of the cells to tumor sites, but accelerated the clearance of IV administered MAK cells from the pulmonary circulation.[108]

Cell labeling using ^{99m}Tc-HMPAO

Similar to leukocyte labeling, monocytes have been labeled with ^{99m}Tc-HMPAO for the purpose of infection and inflammation imaging.[109] To our knowledge, no application of ^{99m}Tc-HMPAO in cancer imaging has been reported.

Passive incorporation of the cell membrane

The lipophilic tracer 1,1-dioctadecyl-3,3,3,3-tetramethylindotricarbocyanine iodide (DiR), used in near infrared (NIR) imaging is passively incorporated in the lipid bilayer of the cell membrane. One advantage of the use of near infrared imaging is that it has relatively low noise. Eisenblätter *et al.* used prelabeled macrophages with DiR to localize inflammation in a mouse model with cutaneous granuloma and measured the signal with two NIR imaging techniques; fluorescence reflectance imaging and fluorescence-mediated tomography. In this study they found a linear correlation between the number of cells injected intravenously and the signal obtained with NIR imaging.[110] The lack of ionizing radiation and signal decay offers potential of such approach for cancer research.

Active uptake via endogenous transporters

Cell labeling using Glut1

The highly plastic nature of macrophages results in a plethora of phenotypes, with bioenergetic profiles according to the specific environmental stimuli.[111] Pro-inflammatory macrophages are heavily dependent on aerobic glycolysis, whereas macrophages with a tissue-repair phenotype rely on oxidative phosphorylation. As such, TAMs might contribute significantly to the total tumor glycolysis.[112-114] However, to accurately attribute ^{18}F-FDG uptake in the tumor microenvironment to either tumor cells or TAMs remains challenging. In a clinical trial preoperative ^{18}F-FDG PET imaging in 55 breast cancer patients was compared to histochemical staining for macrophage markers on tumor sections.[115] No correlation between ^{18}F-FDG-uptake and presence of macrophages was noted. TAMs have high prognostic impact in classical Hodgkin lymphoma,[116] but studies that correlate early response to treatment as measured by ^{18}F-FDG PET with the presence of CD68$^+$ TAM

populations yield conflicting results,[117, 118] perhaps indicating that the pan-macrophage marker CD68 does not sufficiently reflect the functional orientation of TAMs in cancer.

Interesting approaches, that use pharmacological editing of cellular metabolism to increase the difference in glycolysis in tumor cells *versus* TAMs, have recently been reported. The peroxisome proliferator-activated receptor-gamma (PPARγ), member of the nuclear receptor superfamily of ligand-dependent transcription factors, has been shown to have an anti-inflammatory effect. The PPARγ agonist pioglitazone was studied in a macrophage cell line (RAW264.7) and three tumor cell lines (A549, KB, and MDA-MB-231). After treatment with pioglitazone, the uptake of ^{18}F-FDG in the macrophages was decreased and uptake of ^{18}F-FDG in the tumor cells was increased. Unlike tumors, the RAW264.7 xenograft model showed the reduced ^{18}F-FDG uptake in the inflammatory lesion from 11.74±1.19 to 6.50±1.47 (%ID/g). The increase in ^{18}F-FDG in the different tumor cell lines was less profound.[119] Similar findings are reported for rosiglitazone.[120] In preclinical models on atherosclerosis, intravenous injections of GM-CSF increased detection by ^{18}F-FDG PET, by augmenting the glycolytic flux within inflamed atheroma *in vivo*, demonstrating that GM-CSF can be used to enhance detection of inflammation.[121]

Cell labeling using TSPO

Originally discovered as peripheral benzodiazepine receptor in cells of the central nervous system, with high affinity binding of diazepam, this mitochondrial receptor was renamed to "translocator protein-18 kDa" (TSPO). The most studied function of TSPO is in steroid synthesis through regulation of cholesterol transport from the outer to the inner mitochondrial membranes, especially in activated microglial cells and macrophages. As such it is a target for PET imaging of neuroinflammation using isoquinoline carboxamide derivative R-[N-methyl-^{11}CPK-11195 as prototype tracer. In twenty-two patients with glioma, dynamic ^{11}C-(R)PK11195 imaging was performed.[122] Tracer binding potential in high-grade gliomas was significantly higher than in low-grade astrocytomas, and correlated with the expression of TSPO in the tumor. However, TAMs only partially contributed to the overall TSPO expression, and TSPO expression in TAMs did not correlate with PET imaging. To the contrary, high TSPO expression was measured in 20/25 (80%) of the patient-derived breast cancer xenografts.[123] Immunohistochemistry showed that a significant portion of the tumor stromal TSPO expression co-localized with F4/80 positive macrophages cells. ^{18}F-N-(2-(2-fluoroethoxy)benzyl)-N-(4-phenoxypyridin-3-yl)acetamide (^{18}F-FEPPA). Tumor uptake of ^{18}F-FEPPA in mice bearing subcutaneous MDA-MB-231 breast cancer xenografts was evaluated by PET imaging and *ex-vivo* biodistribution studies. Although the tumor was successfully visualized, *ex-vivo* biodistribution studies revealed low tumor uptake (0.7%ID/g), with the majority of radioactivity distributed in the spleen, muscle, and heart despite high TSPO expression in this cell line.[124] To our knowledge, no clinical studies on imaging of TAMs by targeting TSPO have been reported.

Active uptake via endocytic pathways

Cell labeling using LDL

Radiolabeled rHDL nanoparticles loaded with ^{89}Zr have been evaluated in an orthotopic mouse model of breast cancer to specifically image TAMs. Two variants of the nanoparticles were investigated; phospholipid- and apoA-I-labeled rHDL and both probes resulted in high tumor accumulation (16.5±2.8 and 8.6±1.3 %ID/g, respectively) at 24 hours after injection. Histologic analysis demonstrated good co-localization of radioactivity with TAM-rich areas in tumor sections. Furthermore, flow cytometry analyses showed high uptake of rHDL nanoparticles per cell (6.8-fold higher in TAMs than in tumor cells for both nanoparticles) and accounted for nearly 50% of the total accumulated activity in the tumor lesion.[125]

Cell labeling using nanoparticles

Macrophages display a wide array of means for engulfing particles from the microenvironment, including phagocytosis, endocytosis and pinocytosis. For imaging purposes, nanoparticles have experienced great interest in the recent years, as nanoparticles can be modulated to optimize tissue distribution (size, charge, coating)

or cellular distribution (coating, targeting moieties), and can be loaded with a variety of (multimodal) contrast agents.[126] As such, nanoparticles provide efficient scaffolds for *in-vivo* or *ex-vivo* labeling of macrophages.[38, 39, 74]

For example, PLGA-based nanoparticles of 200 nm in size can be loaded with ^{19}F, as well as different fluorescent dyes for tracking even relatively non-phagocytic dendritic cells: human myeloid and plasmacytoid dendritic cells. Using these different fluorescence labels, simultaneous imaging of distinct immune cell populations is feasible on a clinical 3T MR scanner with reasonable acquisition times. The estimated sensitivity was 2 million cells/MRS voxel for non-phagocytic cells and 200,000 cells for highly phagocytic cells, *e.g.* monocyte-derived dendritic cells, which would be sufficient for clinical studies.[127]

Including a radionuclide for PET imaging would potentially improve the sensitivity of detecting nanoparticle-labeled TAMs to allow whole body imaging.[128, 129] Cross-linked dextran nanoparticles, of 13 nm in size, have been labeled with ^{89}Zr and injected IV in a CT26 mouse tumor model to target TAMs.[130] Phenotyping the *in-vivo* labeled TAM populations isolated from the tumor revealed a rather unspecific targeting of populations of $Ly6C^{hi}$, $Ly6C^{lo}$ and $F4/80^{hi}$ cells. However, tumors could successfully be visualized with <5% of the injected dose needed for MR imaging.

Cell labeling using (U)SPIO

(U)SPIO nanoparticles are clinically approved for lymph node staging on MR, based on the uptake of particles that have diffused into the interstitial space by phagocytic myeloid cells.[129] In a series of experiments, Daldrup-Link *et al.* compared the clinical compound with optimized SPIOs for imaging TAMs. $F4/80^{+}$ mouse macrophages were labeled *ex vivo* with ferumoxytol, a dextran coated 30-nm nanoparticle; P904, a hydrophilic-coated 21-nm nanoparticle, or P1133, a hydrophilic coated plus folate 26-nm nanoparticle.[131] They showed improved uptake *ex vivo* and increased change in R2 signal on MR imaging with folate coated nanoparticles at 24 hours post-injection, suggesting that modifications of the coating can optimize cellular uptake of nanoparticles.

Active uptake via specific receptors

Cell labeling targeting the mannose receptor

Along with the highly diverse and plastic phenotype of TAMs, heterogeneity in intratumoral niches imply differentially orientated TAMs that express specific receptors. Pro-angiogenic TAMs that reside in hypoxic tumor areas for example express macrophage mannose receptor (MMR, CD206). This receptor can be targeted with nanobodies, which are single-domain antigen-binding fragments derived from *Camelidae* heavy-chain antibodies. MMR-specific nanobodies stained TAMs in lung and breast tumor single-cell suspensions *in vitro*. In a preclinical model, intravenous injection of ^{99m}Tc-labeled anti-MMR nanobodies successfully targeted tumor *in vivo*. Retention of the nanobody was receptor-specific and absent in MMR-deficient mice. To enhance signal-to-background ratios, co-injection of unlabeled anti-MMR nanobodies reduced to background uptake in normal organs, without compromising tumor uptake. Further, anti-MMR nanobodies accumulated in hypoxic regions, thus supporting the hypothesis that pro-angiogenic TAMs were targeted.[132] Following the same principle, a PET tracer ^{18}F-fluorobenzoate (FB)-anti-MMR nanobody was developed using the prosthetic group N-succinimidyl-4-^{18}F-fluorobenzoate (^{18}F-SFB). The kidney retention of the fluorinated nanobody was 20-fold lower than a ^{99m}Tc-labeled counterpart. Compared with MMR- and CCR2-deficient mice, significantly higher uptake was observed in tumors grown in wild-type mice.[133]

Conclusion and future directions

In-vivo imaging faces the challenge to image specific subsets of immune cells, which are present only in small absolute numbers in cancer lesions and display a highly dynamic behavior. The contemporary imaging toolbox for researchers, as well as clinicians, provides a diverse range of possible imaging modalities and tracers. The most optimal combination of radionuclide/contrast agent, tracer and thus imaging modality highly depends on the hypothesis and involved immune cell population under question. This review aimed to provide arguments that can guide the design of an *in-vivo* imaging study on tumor-infiltrating immune cells in both preclinical and clinical setting.

Recent developments, mentioned below, are foreseen to play a critical role in the optimization and individualization of anti-cancer therapy in the near future.

Multimodal imaging

It would be simplistic to expect that the complex interactions of both tissue resident stromal and recruited immune cells with the heterogeneous population of cancer cells can be evaluated by assessing a single parameter. The stringent requirements for an imaging approach to evaluate tumor-infiltrating immune cells can currently only be met exploiting multiple modalities. DCE and DW MR imaging is increasingly being used to evaluate tissue changes to therapy at ultra-high resolution, it allows measures of plasma volume fraction/micro vessel density (fpV), vessel permeability (K_{trans} and k_{ep}), cellularity (apparent diffusion coefficient). The inflammatory responses elicited by anti-cancer therapy are known to induce these changes, prior to shrinkage of tumor volumes, which could help to characterize changes in cellular composition of TME following anti-cancer therapy, in particular in combination with metabolic evaluation of cancer lesions with ^{18}F-FDG PET.

Antibody fragments, peptides and small molecules

Considering the high specificity of radiolabeled mAbs, effort have been made to increase the specific targeting of immune cells by using smaller antibody fragments, like "minibodies," "diabodies" or scFv's, peptides and small molecules which have a more rapid tissue penetration, rapid clearance and generally reveal higher target-to-background ratios. Together with using PET radionuclides such as ^{18}F or ^{68}Ga, these agents could improve image quality to clinically relevant levels, which will boost *in-vivo* imaging. To this end, careful evaluation of possible effect of tracers on labeled immune cells, in particular labeling-induced exhaustion and interactions with other cells in the TME, is urgent.

Selecting therapeutic targets

Radiolabeled mAbs targeting disease-specific processes are likely to have increasing impact on treatment stratification. For example, antibodies blocking the PD1-PDL-1 axis have shown impressive results in various types of cancer, and patients with high expression of PDL-1 are most likely to benefit from this therapy. Heskamp *et al.* developed an ^{111}In-labeled anti-PDL-1 antibody with accumulation in PD-L1 expressing tumors and no specific uptake was observed in tumors with low or no detectable levels of PD-L1. Moreover, SPECT/CT and autoradiography showed a heterogeneous distribution of ^{111}In-PD-L1 within the tumor, which might be worthwhile to explore in future studies. The recent development on "small engineered protein" radiotracers highlights the current interest in imaging human immune checkpoints.

Advanced image analysis

Heterogeneity within cancer lesions has long been recognized from clinical images, however accurate measures to interpret particular patterns were lacking. Intra-tumoral heterogeneity plays an important role in immune cell imaging, since the infiltration of immune cell populations can be very heterogeneously distributed within the tumor, which potentially hints on their role in the microenvironment. Improved algorithms to classify regions of tumor tissue and to extract as much data from both PET and MR scan images are now opening up avenues for validation in clinical settings. *In-vivo* defining the metabolic and functional profiles of tumors on molecular, cellular and tissue level has the potential to consolidate imaging technology as most valuable tool in the field of cancer treatment.

References

1. Senovilla L, Vacchelli E, Galon J, Adjemian S, Eggermont A, Fridman WH, *et al.* Trial watch: Prognostic and predictive value of the immune infiltrate in cancer. Oncoimmunology 2012;1:1323-43.
2. Fridman WH, Pages F, Sautes-Fridman C, Galon J. The immune contexture in human tumours: impact on clinical outcome. Nat Rev Cancer 2012;12:298-306.
3. Galon J, Costes A, Sanchez-Cabo F, Kirilovsky A, Mlecnik B, Lagorce-Pages C, *et al.* Type, density, and location of immune cells within human colorectal tumors predict clinical outcome. Science 2006;313:1960-4.
4. Ngiow SF, Young A, Jacquelot N, Yamazaki T, Enot D, Zitvogel L, *et al.* A Threshold Level of Intratumor CD8+ T-cell PD1 Expression Dictates Therapeutic Response to Anti-PD1. Cancer Res 2015;75:3800-11.
5. Giraldo NA, Becht E, Vano Y, Sautes-Fridman C, Fridman WH. The immune response in cancer: from immunology to pathology to immunotherapy. Virchows Arch 2015;467:127-35.
6. Taube JM, Young GD, McMiller TL, Chen S, Salas JT, Pritchard TS, *et al.* Differential Expression of Immune-Regulatory Genes Associated with PD-L1 Display in Melanoma: Implications for PD-1 Pathway Blockade. Clin Cancer Res 2015;21:3969-76.

7. Tumeh PC, Harview CL, Yearley JH, Shintaku IP, Taylor EJ, Robert L, *et al.* PD-1 blockade induces responses by inhibiting adaptive immune resistance. Nature 2014;515:568-71.
8. Church SE, Galon J. Tumor Microenvironment and Immunotherapy: The Whole Picture Is Better Than a Glimpse. Immunity 2015;43:631-3.
9. Holzel M, Bovier A, Tuting T. Plasticity of tumour and immune cells: a source of heterogeneity and a cause for therapy resistance? Nat Rev Cancer 2013;13:365-76.
10. Bindea G, Mlecnik B, Tosolini M, Kirilovsky A, Waldner M, Obenauf AC, *et al.* Spatiotemporal dynamics of intratumoral immune cells reveal the immune landscape in human cancer. Immunity 2013;39:782-95.
11. Wolfs E, Verfaillie CM, Van Laere K, Deroose CM. Radiolabeling strategies for radionuclide imaging of stem cells. Stem Cell Rev 2015;11:254-74.
12. Nguyen PK, Riegler J, Wu JC. Stem cell imaging: from bench to bedside. Cell Stem Cell 2014;14:431-44.
13. Naumova AV, Modo M, Moore A, Murry CE, Frank JA. Clinical imaging in regenerative medicine. Nat Biotechnol 2014;32:804-18.
14. James ML, Gambhir SS. A molecular imaging primer: modalities, imaging agents, and applications. Physiol Rev 2012;92:897-965.
15. Moroz MA, Zhang H, Lee J, Moroz E, Zurita J, Shenker L, *et al.* Comparative Analysis of T Cell Imaging with Human Nuclear Reporter Genes. J Nucl Med 2015;56:1055-60.
16. Thakur ML, Lavender JP, Arnot RN, Silvester DJ, Segal AW. Indium-111-labeled autologous leukocytes in man. J Nucl Med 1977;18:1014-21.
17. Danpure HJ, Osman S. Optimum conditions for radiolabelling human granulocytes and mixed leucocytes with 111In-tropolonate. Eur J Nucl Med 1988;13:537-42.
18. Chin BB, Nakamoto Y, Bulte JW, Pittenger MF, Wahl R, Kraitchman DL. 111In oxine labelled mesenchymal stem cell SPECT after intravenous administration in myocardial infarction. Nucl Med Commun 2003;24:1149-54.
19. Gholamrezanezhad A, Mirpour S, Ardekani JM, Bagheri M, Alimoghadam K, Yarmand S, *et al.* Cytotoxicity of 111In-oxine on mesenchymal stem cells: a time-dependent adverse effect. Nucl Med Commun 2009;30:210-6.
20. Gildehaus FJ, Haasters F, Drosse I, Wagner E, Zach C, Mutschler W, *et al.* Impact of indium-111 oxine labelling on viability of human mesenchymal stem cells in vitro, and 3D cell-tracking using SPECT/CT in vivo. Mol Imaging Biol 2011;13:1204-14.
21. Nowak B, Weber C, Schober A, Zeiffer U, Liehn EA, von Hundelshausen P, *et al.* Indium-111 oxine labelling affects the cellular integrity of haematopoietic progenitor cells. Eur J Nucl Med Mol Imaging 2007;34:715-21.
22. Balaban EP, Simon TR, Frenkel EP. Toxicity of indium-111 on the radiolabeled lymphocyte. J Nucl Med 1987;28:229-33.
23. Signore A, Sensi M, Pozzilli C, Negri M, Lenzi GL, Pozzilli P. Effect of unlabeled indium oxine and indium tropolone on the function of isolated human lymphocytes. J Nucl Med 1985;26:612-5.
24. de Vries EF, Roca M, Jamar F, Israel O, Signore A. Guidelines for the labelling of leucocytes with (99m)Tc-HMPAO. Inflammation/Infection Taskgroup of the European Association of Nuclear Medicine. Eur J Nucl Med Mol Imaging 2010;37:842-8.
25. Adonai N, Nguyen KN, Walsh J, Iyer M, Toyokuni T, Phelps ME, *et al.* Ex vivo cell labeling with 64Cu-pyruvaldehyde-bis(N4-methylthiosemicarbazone) for imaging cell trafficking in mice with positron-emission tomography. Proc Natl Acad Sci U S A 2002;99:3030-5.
26. Blower PJ, Lewis JS, Zweit J. Copper radionuclides and radiopharmaceuticals in nuclear medicine. Nucl Med Biol 1996;23:957-80.
27. Prince HM, Wall DM, Ritchie D, Honemann D, Harrrison S, Quach H, *et al.* In vivo tracking of dendritic cells in patients with multiple myeloma. J Immunother 2008;31:166-79.
28. Griessinger CM, Kehlbach R, Bukala D, Wiehr S, Bantleon R, Cay F, *et al.* In vivo tracking of Th1 cells by PET reveals quantitative and temporal distribution and specific homing in lymphatic tissue. J Nucl Med 2014;55:301-7.
29. Bindslev L, Haack-Sorensen M, Bisgaard K, Kragh L, Mortensen S, Hesse B, *et al.* Labelling of human mesenchymal stem cells with indium-111 for SPECT imaging: effect on cell proliferation and differentiation. Eur J Nucl Med Mol Imaging 2006;33:1171-7.
30. Danpure HJ, Osman S. The importance of radiolabelling human granulocytes with 111In-tropolonate or 111In-2-mercaptopyridine-N-oxide in plasma containing acid-citrate-dextrose. Br J Radiol 1986;59:907-10.
31. Danpure HJ, Osman S, Brady F. The labelling of blood cells in plasma with 111In-tropolonate. Br J Radiol 1982;55:247-9.
32. Bansal A, Pandey MK, Demirhan YE, Nesbitt JJ, Crespo-Diaz RJ, Terzic A, *et al.* Novel (89)Zr cell labeling approach for PET-based cell trafficking studies. EJNMMI Res 2015;5:19.
33. Ma B, Hankenson KD, Dennis JE, Caplan AI, Goldstein SA, Kilbourn MR. A simple method for stem cell labeling with fluorine 18. Nucl Med Biol 2005;32:701-5.
34. Lacroix S, Egrise D, Van Simaeys G, Doumont G, Monclus M, Sherer F, *et al.* [18F]-FBEM, a tracer targeting cell-surface protein thiols for cell trafficking imaging. Contrast Media Mol Imaging 2013;8:409-16.
35. Pearce EL, Poffenberger MC, Chang CH, Jones RG. Fueling immunity: insights into metabolism and lymphocyte function. Science 2013;342:1242454.
36. Bhargava KK, Gupta RK, Nichols KJ, Palestro CJ. In vitro human leukocyte labeling with (64)Cu: an intraindividual comparison with (111)In-oxine and (18)F-FDG. Nucl Med Biol 2009;36:545-9.
37. Stojanov K, de Vries EF, Hoekstra D, van Waarde A, Dierckx RA, Zuhorn IS. [18F]FDG labeling of neural stem cells for in vivo cell tracking with positron emission tomography: inhibition of tracer release by phloretin. Mol Imaging 2012;11:1-12.
38. Weissleder R, Nahrendorf M, Pittet MJ. Imaging macrophages with nanoparticles. Nat Mater 2014;13:125-38.
39. Srinivas M, Boehm-Sturm P, Figdor CG, de Vries IJ, Hoehn M. Labeling cells for in vivo tracking using (19)F MRI. Biomaterials 2012;33:8830-40.
40. Getts DR, Shea LD, Miller SD, King NJ. Harnessing nanoparticles for immune modulation. Trends Immunol 2015;36:419-27.
41. Harisinghani MG, Barentsz J, Hahn PF, Deserno WM, Tabatabaei S, van de Kaa CH, *et al.* Noninvasive detection of clinically occult lymph-node metastases in prostate cancer. N Engl J Med 2003;348:2491-9.
42. de Vries IJ, Lesterhuis WJ, Barentsz JO, Verdijk P, van Krieken JH, Boerman OC, *et al.* Magnetic resonance tracking of dendritic cells in melanoma patients for monitoring of cellular therapy. Nat Biotechnol 2005;23:1407-13.
43. Schroth HJ, Oberhausen E, Berberich R. Cell labelling with colloidal substances in whole blood. Eur J Nucl Med 1981;6:469-72.
44. Segall GM, Lang EV, Chaovapong W. In vitro evaluation of white blood cell labelling with 99Tcm radiopharmaceuticals. Nucl Med Commun 1994;15:845-9.
45. Nadkarni GD, Shimpi HH, Noronha OP. Binding of 99Tcm sulphur colloid to blood components: implications in renal transplant rejection. Nucl Med Commun 1988;9:899-905.
46. McAfee JG, Thakur ML. Survey of radioactive agents for in vitro labeling of phagocytic leukocytes. I. Soluble agents. J Nucl Med 1976;17:480-7.
47. Hanna RW, Lomas FE. Identification of factors affecting technetium 99m leucocyte labelling by phagocytic engulfment and development of an optimal technique. Eur J Nucl Med 1986;12:159-62.
48. Malviya G, Galli F, Sonni I, Signore A. Imaging T-lymphocytes in inflammatory diseases: a nuclear medicine approach. Q J Nucl Med Mol Imaging 2014;58:237-57.
49. Tavare R, Escuin-Ordinas H, Mok S, McCracken MN, Zettlitz KA, Salazar FB, *et al.* An Effective Immuno-PET Imaging Method to Monitor CD8-Dependent Responses to Immunotherapy. Cancer Res 2016;76:73-82.
50. Tarantal AF, Lee CC, Kukis DL, Cherry SR. Radiolabeling human peripheral blood stem cells for positron emission tomography (PET) imaging in young rhesus monkeys. PLoS One 2013;8:e77148.

51. Meijs WE, Herscheid JD, Haisma HJ, Pinedo HM. Evaluation of desferal as a bifunctional chelating agent for labeling antibodies with Zr-89. Int J Rad Appl Instrum A 1992;43:1443-7.
52. Vugts DJ, Klaver C, Sewing C, Poot AJ, Adamzek K, Huegli S, *et al.* Comparison of the octadentate bifunctional chelator DFO*-pPhe-NCS and the clinically used hexadentate bifunctional chelator DFO-pPhe-NCS for (89)Zr-immuno-PET. Eur J Nucl Med Mol Imaging 2017;44:286-95.
53. Kircher MF, Gambhir SS, Grimm J. Noninvasive cell-tracking methods. Nat Rev Clin Oncol 2011;8:677-88.
54. Acton PD, Zhou R. Imaging reporter genes for cell tracking with PET and SPECT. Q J Nucl Med Mol Imaging 2005;49:349-60.
55. Moore A, Josephson L, Bhorade RM, Basilion JP, Weissleder R. Human transferrin receptor gene as a marker gene for MR imaging. Radiology 2001;221:244-50.
56. Gambhir SS, Barrio JR, Wu L, Iyer M, Namavari M, Satyamurthy N, *et al.* Imaging of adenoviral-directed herpes simplex virus type 1 thymidine kinase reporter gene expression in mice with radiolabeled ganciclovir. J Nucl Med 1998;39:2003-11.
57. Grimfors GG. Tumour imaging of indium-111 oxine-labelled autologous lymphocytes as a staging method in Hodgkin's disease. European journal of haematology 1989;42:276-83.
58. Fisher B, Packard BS, Read EJ, Carrasquillo JA, Carter CS, Topalian SL, *et al.* Tumor localization of adoptively transferred indium-111 labeled tumor infiltrating lymphocytes in patients with metastatic melanoma. J Clin Oncol 1989;7:250-61.
59. Griffith KD, Read EJ, Carrasquillo JA, Carter CS, Yang JC, Fisher B, *et al.* In vivo distribution of adoptively transferred indium-111-labeled tumor infiltrating lymphocytes and peripheral blood lymphocytes in patients with metastatic melanoma. J Natl Cancer Inst 1989;81:1709-17.
60. Pittet MJ, Grimm J, Berger CR, Tamura T, Wojtkiewicz G, Nahrendorf M, *et al.* In vivo imaging of T cell delivery to tumors after adoptive transfer therapy. Proc Natl Acad Sci U S A 2007;104:12457-61.
61. Sharif-Paghaleh E, Leech J, Sunassee K, Ali N, Sagoo P, Lechler RI, *et al.* Monitoring the efficacy of dendritic cell vaccination by early detection of (99m) Tc-HMPAO-labelled CD4(+) T cells. Eur J Immunol 2014;44:2188-91.
62. Charoenphun P, Meszaros LK, Chuamsaamarkkee K, Sharif-Paghaleh E, Ballinger JR, Ferris TJ, *et al.* [(89)Zr]oxinate4 for long-term in vivo cell tracking by positron emission tomography. Eur J Nucl Med Mol Imaging 2015;42:278-87.
63. Sato N, Wu H, Asiedu KO, Szajek LP, Griffiths GL, Choyke PL. (89)Zr-Oxine Complex PET Cell Imaging in Monitoring Cell-based Therapies. Radiology 2015;275:490-500.
64. Bhatnagar P, Li Z, Choi Y, Guo J, Li F, Lee DY, *et al.* Imaging of genetically engineered T cells by PET using gold nanoparticles complexed to Copper-64. Integr Biol (Camb) 2013;5:231-8.
65. Bondue B, Sherer F, Van Simaeys G, Doumont G, Egrise D, Yakoub Y, *et al.* PET/CT with 18F-FDG- and 18F-FBEM-labeled leukocytes for metabolic activity and leukocyte recruitment monitoring in a mouse model of pulmonary fibrosis. J Nucl Med 2015;56:127-32.
66. Botti C, Negri DR, Seregni E, Ramakrishna V, Arienti F, Maffioli L, *et al.* Comparison of three different methods for radiolabelling human activated T lymphocytes. Eur J Nucl Med 1997;24:497-504.
67. Shields AF, Grierson JR, Dohmen BM, Machulla HJ, Stayanoff JC, Lawhorn-Crews JM, *et al.* Imaging proliferation in vivo with [F-18]FLT and positron emission tomography. Nat Med 1998;4:1334-6.
68. Aarntzen EH, Srinivas M, De Wilt JH, Jacobs JF, Lesterhuis WJ, Windhorst AD, *et al.* Early identification of antigen-specific immune responses in vivo by [18F]-labeled 3'-fluoro-3'-deoxythymidine ([18F]FLT) PET imaging. Proc Natl Acad Sci U S A 2011;108:18396-9.
69. Van Rompay AR, Johansson M, Karlsson A. Substrate specificity and phosphorylation of antiviral and anticancer nucleoside analogues by human deoxyribonucleoside kinases and ribonucleoside kinases. Pharmacol Ther 2003;100:119-39.
70. Radu CG, Shu CJ, Nair-Gill E, Shelly SM, Barrio JR, Satyamurthy N, *et al.* Molecular imaging of lymphoid organs and immune activation by positron emission tomography with a new [18F]-labeled 2'-deoxycytidine analog. Nat Med 2008;14:783-8.
71. Kang J, Zhu L, Lu J, Zhang X. Application of metabolomics in autoimmune diseases: insight into biomarkers and pathology. J Neuroimmunol 2015;279:25-32.
72. Kadayakkara DK, Beatty PL, Turner MS, Janjic JM, Ahrens ET, Finn OJ. Inflammation driven by overexpression of the hypoglycosylated abnormal mucin 1 (MUC1) links inflammatory bowel disease and pancreatitis. Pancreas 2010;39:510-5.
73. Nam HY, Kwon SM, Chung H, Lee SY, Kwon SH, Jeon H, *et al.* Cellular uptake mechanism and intracellular fate of hydrophobically modified glycol chitosan nanoparticles. J Control Release 2009;135:259-67.
74. Ahrens ET, Bulte JW. Tracking immune cells in vivo using magnetic resonance imaging. Nat Rev Immunol 2013;13:755-63.
75. Smirnov P, Lavergne E, Gazeau F, Lewin M, Boissonnas A, Doan BT, *et al.* In vivo cellular imaging of lymphocyte trafficking by MRI: a tumor model approach to cell-based anticancer therapy. Magn Reson Med 2006;56:498-508.
76. Kircher MF, Allport JR, Graves EE, Love V, Josephson L, Lichtman AH, *et al.* In vivo high resolution three-dimensional imaging of antigen-specific cytotoxic T-lymphocyte trafficking to tumors. Cancer Res 2003;63:6838-46.
77. Thu MS, Bryant LH, Coppola T, Jordan EK, Budde MD, Lewis BK, *et al.* Self-assembling nanocomplexes by combining ferumoxytol, heparin and protamine for cell tracking by magnetic resonance imaging. Nat Med 2012;18:463-7.
78. Janjic JM, Ahrens ET. Fluorine-containing nanoemulsions for MRI cell tracking. Wiley Interdiscip Rev Nanomed Nanobiotechnol 2009;1:492-501.
79. Janjic JM, Srinivas M, Kadayakkara DK, Ahrens ET. Self-delivering nanoemulsions for dual fluorine-19 MRI and fluorescence detection. J Am Chem Soc 2008;130:2832-41.
80. Pittet MJ, Swirski FK, Reynolds F, Josephson L, Weissleder R. Labeling of immune cells for in vivo imaging using magnetofluorescent nanoparticles. Nat Protoc 2006;1:73-9.
81. Bhatnagar P, Alauddin M, Bankson JA, Kirui D, Seifi P, Huls H, *et al.* Tumor lysing genetically engineered T cells loaded with multimodal imaging agents. Sci Rep 2014;4:4502.
82. Signore A, Chianelli M, Toscano A, Monetini L, Ronga G, Nimmon CC, *et al.* A radiopharmaceutical for imaging areas of lymphocytic infiltration: 123I-interleukin-2. Labelling procedure and animal studies. Nucl Med Commun 1992;13:713-22.
83. Chianelli M, Signore A, Fritzberg AR, Mather SJ. The development of technetium-99m-labelled interleukin-2: a new radiopharmaceutical for the in vivo detection of mononuclear cell infiltrates in immune-mediated diseases. Nucl Med Biol 1997;24:579-86.
84. Zhang M, Yao Z, Garmestani K, Yu S, Goldman CK, Paik CH, *et al.* Preclinical evaluation of an anti-CD25 monoclonal antibody, 7G7/B6, armed with the beta-emitter, yttrium-90, as a radioimmunotherapeutic agent for treating lymphoma. Cancer Biother Radiopharm 2009;24:303-9.
85. Tavare R, McCracken MN, Zettlitz KA, Salazar FB, Olafsen T, Witte ON, *et al.* Immuno-PET of Murine T Cell Reconstitution Postadoptive Stem Cell Transplantation Using Anti-CD4 and Anti-CD8 Cys-Diabodies. J Nucl Med 2015;56:1258-64.
86. Mall S, Yusufi N, Wagner R, Klar R, Bianchi H, Steiger K, *et al.* Immuno-PET Imaging of Engineered Human T Cells in Tumors. Cancer Res 2016;76:4113-23.
87. Yaghoubi SS, Campbell DO, Radu CG, Czernin J. Positron emission tomography reporter genes and reporter probes: gene and cell therapy applications. Theranostics 2012;2:374-91.
88. Yaghoubi SS, Jensen MC, Satyamurthy N, Budhiraja S, Paik D, Czernin J, *et al.* Noninvasive detection of therapeutic cytolytic T cells with 18F-FHBG PET in a patient with glioma. Nat Clin Pract Oncol 2009;6:53-8.
89. Campbell DO, Yaghoubi SS, Su Y, Lee JT, Auerbach MS, Her-

schman H, *et al.* Structure-guided engineering of human thymidine kinase 2 as a positron emission tomography reporter gene for enhanced phosphorylation of non-natural thymidine analog reporter probe. J Biol Chem 2012;287:446-54.
90. McCracken MN, Vatakis DN, Dixit D, McLaughlin J, Zack JA, Witte ON. Noninvasive detection of tumor-infiltrating T cells by PET reporter imaging. J Clin Invest 2015;125:1815-26.
91. Meller B, Frohn C, Brand JM, Lauer I, Schelper LF, von Hof K, *et al.* Monitoring of a new approach of immunotherapy with allogenic (111)In-labelled NK cells in patients with renal cell carcinoma. Eur J Nucl Med Mol Imaging 2004;31:403-7.
92. Brand JM, Meller B, Von Hof K, Luhm J, Bahre M, Kirchner H, *et al.* Kinetics and organ distribution of allogeneic natural killer lymphocytes transfused into patients suffering from renal cell carcinoma. Stem Cells Dev 2004;13:307-14.
93. Cany J, van der Waart AB, Tordoir M, Franssen GM, Hangalapura BN, de Vries J, *et al.* Natural killer cells generated from cord blood hematopoietic progenitor cells efficiently target bone marrow-residing human leukemia cells in NOD/SCID/IL2Rg(null) mice. PLoS One 2013;8:e64384.
94. Malviya G, Nayak T, Gerdes C, Dierckx RA, Signore A, de Vries EF. Isolation and (111)In-Oxine Labeling of Murine NK Cells for Assessment of Cell Trafficking in Orthotopic Lung Tumor Model. Mol Pharm 2016;13:1329-38.
95. Tavri S, Jha P, Meier R, Henning TD, Muller T, Hostetter D, *et al.* Optical imaging of cellular immunotherapy against prostate cancer. Mol Imaging 2009;8:15-26.
96. Meier R, Piert M, Piontek G, Rudelius M, Oostendorp RA, Senekowitsch-Schmidtke R, *et al.* Tracking of [18F]FDG-labeled natural killer cells to HER2/neu-positive tumors. Nucl Med Biol 2008;35:579-88.
97. Mallett CL, McFadden C, Chen Y, Foster PJ. Migration of iron-labeled KHYG-1 natural killer cells to subcutaneous tumors in nude mice, as detected by magnetic resonance imaging. Cytotherapy 2012;14:743-51.
98. Bouchlaka MN, Ludwig KD, Gordon JW, Kutz MP, Bednarz BP, Fain SB, *et al.* (19)F-MRI for monitoring human NK cells in vivo. Oncoimmunology 2016;5:e1143996.
99. Galli F, Rapisarda AS, Stabile H, Malviya G, Manni I, Bonanno E, *et al.* In Vivo Imaging of Natural Killer Cell Trafficking in Tumors. J Nucl Med 2015;56:1575-80.
100. Edinger M, Cao YA, Verneris MR, Bachmann MH, Contag CH, Negrin RS. Revealing lymphoma growth and the efficacy of immune cell therapies using in vivo bioluminescence imaging. Blood 2003;101:640-8.
101. Shand FH, Ueha S, Otsuji M, Koid SS, Shichino S, Tsukui T, *et al.* Tracking of intertissue migration reveals the origins of tumor-infiltrating monocytes. Proc Natl Acad Sci U S A 2014;111:7771-6.
102. Cortez-Retamozo V, Etzrodt M, Newton A, Rauch PJ, Chudnovskiy A, Berger C, *et al.* Origins of tumor-associated macrophages and neutrophils. Proc Natl Acad Sci U S A 2012;109:2491-6.
103. Adams DL, Martin SS, Alpaugh RK, Charpentier M, Tsai S, Bergan RC, *et al.* Circulating giant macrophages as a potential biomarker of solid tumors. Proc Natl Acad Sci U S A 2014;111:3514-9.
104. Clawson GA, Kimchi E, Patrick SD, Xin P, Harouaka R, Zheng S, *et al.* Circulating tumor cells in melanoma patients. PLoS One 2012;7:e41052.
105. Quillien V, Moisan A, Lesimple T, Leberre C, Toujas L. Biodistribution of 111indium-labeled macrophages infused intravenously in patients with renal carcinoma. Cancer Immunol Immunother 2001;50:477-82.
106. Faradji A, Bohbot A, Schmitt-Goguel M, Roeslin N, Dumont S, Wiesel ML, *et al.* Phase I trial of intravenous infusion of ex-vivo-activated autologous blood-derived macrophages in patients with non-small-cell lung cancer: toxicity and immunomodulatory effects. Cancer Immunol Immunother 1991;33:319-26.
107. Andreesen R, Hennemann B, Krause SW. Adoptive immunotherapy of cancer using monocyte-derived macrophages: rationale, current status, and perspectives. J Leukoc Biol 1998;64:419-26.
108. Ritchie D, Mileshkin L, Wall D, Bartholeyns J, Thompson M, Coverdale J, *et al.* In vivo tracking of macrophage activated killer cells to sites of metastatic ovarian carcinoma. Cancer Immunol Immunother 2007;56:155-63.
109. Van Hemert FJ, Voermans C, Van Eck-Smit BL, Bennink RJ. Labeling monocytes for imaging chronic inflammation. Q J Nucl Med Mol Imaging 2009;53:78-88.
110. Eisenblatter M, Ehrchen J, Varga G, Sunderkotter C, Heindel W, Roth J, *et al.* In vivo optical imaging of cellular inflammatory response in granuloma formation using fluorescence-labeled macrophages. J Nucl Med 2009;50:1676-82.
111. Tavakoli S, Zamora D, Ullevig S, Asmis R. Bioenergetic profiles diverge during macrophage polarization: implications for the interpretation of 18F-FDG PET imaging of atherosclerosis. J Nucl Med 2013;54:1661-7.
112. Kubota R, Kubota K, Yamada S, Tada M, Ido T, Tamahashi N. Microautoradiographic study for the differentiation of intratumoral macrophages, granulation tissues and cancer cells by the dynamics of fluorine-18-fluorodeoxyglucose uptake. J Nucl Med 1994;35:104-12.
113. Kubota R, Yamada S, Kubota K, Ishiwata K, Tamahashi N, Ido T. Intratumoral distribution of fluorine-18-fluorodeoxyglucose in vivo: high accumulation in macrophages and granulation tissues studied by microautoradiography. J Nucl Med 1992;33:1972-80.
114. Deichen JT, Prante O, Gack M, Schmiedehausen K, Kuwert T. Uptake of [18F]fluorodeoxyglucose in human monocyte-macrophages in vitro. Eur J Nucl Med Mol Imaging 2003;30:267-73.
115. Bos R, van Der Hoeven JJ, van Der Wall E, van Der Groep P, van Diest PJ, Comans EF, *et al.* Biologic correlates of (18)fluorodeoxyglucose uptake in human breast cancer measured by positron emission tomography. J Clin Oncol 2002;20:379-87.
116. Steidl C, Lee T, Shah SP, Farinha P, Han G, Nayar T, *et al.* Tumor-associated macrophages and survival in classic Hodgkin's lymphoma. N Engl J Med 2010;362:875-85.
117. Cencini E, Fabbri A, Rigacci L, Lazzi S, Gini G, Cox MC, *et al.* Evaluation of the prognostic role of tumour-associated macrophages in newly diagnosed classical Hodgkin lymphoma and correlation with early FDG-PET assessment. Hematol Oncol 2017;35:69-78.
118. Touati M, Delage-Corre M, Monteil J, Abraham J, Moreau S, Remenieras L, *et al.* CD68-positive tumor-associated macrophages predict unfavorable treatment outcomes in classical Hodgkin lymphoma in correlation with interim fluorodeoxyglucose-positron emission tomography assessment. Leuk Lymphoma 2015;56:332-41.
119. Cheong SJ, Lee CM, Kim EM, Lim ST, Sohn MH, Jeong HJ. The effect of PPAR-gamma agonist on (18)F-FDG PET imaging for differentiating tumors and inflammation lesions. Nucl Med Biol 2015;42:85-91.
120. Kim SL, Kim EM, Cheong SJ, Lee CM, Kim DW, Jeong HJ, *et al.* The effect of PPAR-gamma agonist on (18)F-FDG uptake in tumor and macrophages and tumor cells. Nucl Med Biol 2009;36:427-33.
121. Singh P, Gonzalez-Ramos S, Mojena M, Rosales-Mendoza CE, Emami H, Swanson J, *et al.* GM-CSF Enhances Macrophage Glycolytic Activity In Vitro and Improves Detection of Inflammation In Vivo. J Nucl Med 2016;57:1428-35.
122. Su Z, Roncaroli F, Durrenberger PF, Coope DJ, Karabatsou K, Hinz R, *et al.* The 18-kDa mitochondrial translocator protein in human gliomas: an 11C-(R)PK11195 PET imaging and neuropathology study. J Nucl Med 2015;56:512-7.
123. Zheng J, Boisgard R, Siquier-Pernet K, Decaudin D, Dolle F, Tavitian B. Differential expression of the 18 kDa translocator protein (TSPO) by neoplastic and inflammatory cells in mouse tumors of breast cancer. Mol Pharm 2011;8:823-32.
124. Vasdev N, Green DE, Vines DC, McLarty K, McCormick PN, Moran MD, *et al.* Positron-emission tomography imaging of the TSPO with [(18)F]FEPPA in a preclinical breast cancer model. Cancer Biother Radiopharm 2013;28:254-9.
125. Perez-Medina C, Tang J, Abdel-Atti D, Hogstad B, Merad M, Fisher EA, *et al.* PET Imaging of Tumor-Associated Macrophages with

89Zr-Labeled High-Density Lipoprotein Nanoparticles. J Nucl Med 2015;56:1272-7.
126. Welch MJ, Hawker CJ, Wooley KL. The advantages of nanoparticles for PET. J Nucl Med 2009;50:1743-6.
127. Srinivas M, Tel J, Schreibelt G, Bonetto F, Cruz LJ, Amiri H, *et al.* PLGA-encapsulated perfluorocarbon nanoparticles for simultaneous visualization of distinct cell populations by 19F MRI. Nanomedicine (Lond) 2015;10:2339-48.
128. Devaraj NK, Keliher EJ, Thurber GM, Nahrendorf M, Weissleder R. 18F labeled nanoparticles for in vivo PET-CT imaging. Bioconjug Chem 2009;20:397-401.
129. Fukukawa K, Rossin R, Hagooly A, Pressly ED, Hunt JN, Messmore BW, *et al.* Synthesis and characterization of core-shell star copolymers for in vivo PET imaging applications. Biomacromolecules 2008;9:1329-39.
130. Keliher EJ, Yoo J, Nahrendorf M, Lewis JS, Marinelli B, Newton A, *et al.* 89Zr-labeled dextran nanoparticles allow in vivo macrophage imaging. Bioconjug Chem 2011;22:2383-9.
131. Daldrup-Link HE, Golovko D, Ruffell B, Denardo DG, Castaneda R, Ansari C, *et al.* MRI of tumor-associated macrophages with clinically applicable iron oxide nanoparticles. Clin Cancer Res 2011;17:5695-704.
132. Movahedi K, Schoonooghe S, Laoui D, Houbracken I, Waelput W, Breckpot K, *et al.* Nanobody-based targeting of the macrophage mannose receptor for effective in vivo imaging of tumor-associated macrophages. Cancer Res 2012;72:4165-77.
133. Blykers A, Schoonooghe S, Xavier C, D'Hoe K, Laoui D, D'Huyvetter M, *et al.* PET Imaging of Macrophage Mannose Receptor-Expressing Macrophages in Tumor Stroma Using 18F-Radiolabeled Camelid Single-Domain Antibody Fragments. J Nucl Med 2015;56:1265-71.

Authors' contributions.—Carolien Zeelen, Carmen Paus, and Derk Draper have contributed equally to this paper and are joint first authors.

Conflicts of interest.—The authors certify that there is no conflict of interest with any financial organization regarding the material discussed in the manuscript.

Congresses.—This manuscript was partly presented at the Second European Congress on Imaging Infections and Inflammation, which took place on December 12th-13th, 2016, in Rome.

Article first published online: November 30, 2017. - Manuscript accepted: November 29, 2017. - Manuscript received: November 15, 2017.